AMERICAN SOCIETY FOR MICROBIOLOGY | Applied and Environmental Microbiology®

BIODEGRADATION

Biochemical and Genetic Bases of Indole-3-Acetic Acid (Auxin Phytohormone) Degradation by the Plant-Growth-Promoting Rhizobacterium *Paraburkholderia phytofirmans* PsJN

Raúl Donoso,[a,b,c] Pablo Leiva-Novoa,[a,b,c] Ana Zúñiga,[a,b,c] Tania Timmermann,[a,b,c] Gonzalo Recabarren-Gajardo,[d] Bernardo González[a,b,c]

Facultad de Ingeniería y Ciencias, Universidad Adolfo Ibáñez, Santiago, Chile[a]; Millennium Nucleus Center for Plant Systems and Synthetic Biology, Santiago, Chile[b]; Center of Applied Ecology and Sustainability, Santiago, Chile[c]; Departamento de Farmacia, Facultad de Química, Pontificia Universidad Católica de Chile, Santiago, Chile[d]

ABSTRACT Several bacteria use the plant hormone indole-3-acetic acid (IAA) as a sole carbon and energy source. A cluster of genes (named *iac*) encoding IAA degradation has been reported in *Pseudomonas putida* 1290, but the functions of these genes are not completely understood. The plant-growth-promoting rhizobacterium *Paraburkholderia phytofirmans* PsJN harbors *iac* gene homologues in its genome, but with a different gene organization and context than those of *P. putida* 1290. The *iac* gene functions enable *P. phytofirmans* to use IAA as a sole carbon and energy source. Employing a heterologous expression system approach, *P. phytofirmans iac* genes with previously undescribed functions were associated with specific biochemical steps. In addition, two uncharacterized genes, previously unreported in *P. putida* and found to be related to major facilitator and tautomerase superfamilies, are involved in removal of an IAA metabolite called dioxindole-3-acetate. Similar to the case in strain 1290, IAA degradation proceeds through catechol as intermediate, which is subsequently degraded by *ortho*-ring cleavage. A putative two-component regulatory system and a LysR-type regulator, which apparently respond to IAA and dioxindole-3-acetate, respectively, are involved in *iac* gene regulation in *P. phytofirmans*. These results provide new insights about unknown gene functions and complex regulatory mechanisms in IAA bacterial catabolism.

IMPORTANCE This study describes indole-3-acetic acid (auxin phytohormone) degradation in the well-known betaproteobacterium *P. phytofirmans* PsJN and comprises a complete description of genes, some of them with previously unreported functions, and the general basis of their gene regulation. This work contributes to the understanding of how beneficial bacteria interact with plants, helping them to grow and/or to resist environmental stresses, through a complex set of molecular signals, in this case through degradation of a highly relevant plant hormone.

KEYWORDS indole-3-acetic acid catabolism, *iac* genes, *Paraburkholderia phytofirmans*, plant-growth-promoting rhizobacteria

Received 6 July 2016 **Accepted** 14 October 2016

Accepted manuscript posted online 21 October 2016

Citation Donoso R, Leiva-Novoa P, Zúñiga A, Timmermann T, Recabarren-Gajardo G, González B. 2017. Biochemical and genetic bases of indole-3-acetic acid (auxin phytohormone) degradation by the plant-growth-promoting rhizobacterium *Paraburkholderia phytofirmans* PsJN. Appl Environ Microbiol 83:e01991-16. https://doi.org/10.1128/AEM.01991-16.

Editor Rebecca E. Parales, University of California—Davis

Address correspondence to Bernardo González, bernardo.gonzalez@uai.cl.

Indole-3-acetic acid (IAA) belongs to a class of plant hormones called auxins, which play a key role in plant growth and development, controlling cell division, elongation, differentiation, and tropism responses to gravity and light (1, 2). A crucial characteristic of auxin-mediated effects is related to the differential distribution of auxin in tissues (2); therefore, plants tightly control IAA levels through biosynthesis, conjugation, degradation, and intercellular transport (3). Aside from auxin being an essential molecule for

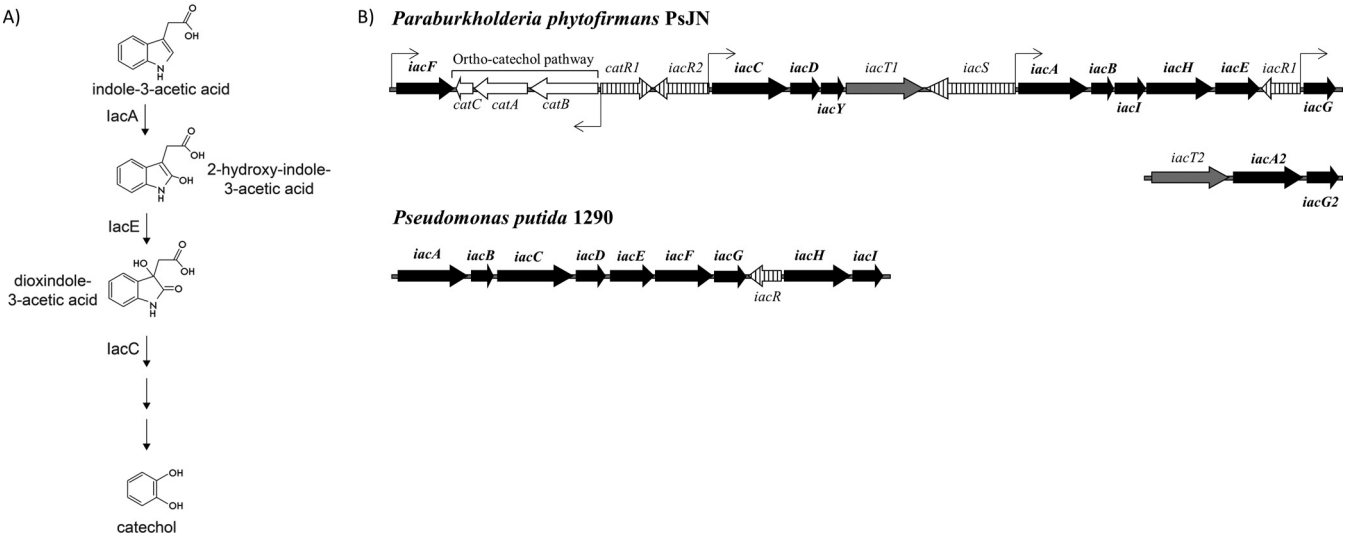

FIG 1 Indole-3-acetic acid (IAA) degradation pathways and gene clusters involved in IAA catabolism in *Paraburkholderia phytofirmans* PsJN and *Pseudomonas putida* 1290. (A) *P. putida* 1290 route channeling IAA to catechol (14), with *iacA*, *iacE*, and *iacC* genes encoding indicated catabolic steps. (Adapted from reference 14.) (B) *iac* genes involved in IAA catabolism. Black arrows indicate putative coding genes directly involved in IAA degradation, gray arrows indicate probable transporters of IAA metabolites, and dashed arrows indicate putative regulators of IAA degradation genes. Genes involved in catechol catabolism are shown in brackets. Thin arrows indicate putative promoter sequences from *iac* genes cloned to construct the corresponding *lacZ* transcriptional fusions.

plants, auxin production is widespread among microorganisms present in soil, water, and plant and animal hosts (4–6). Functions of bacterial IAA synthesis have primarily been associated with plant-microbe interactions, although it has been proposed that they also play a role in interaction with animal hosts and molecular signaling between microorganisms (4–6). Not only do bacteria have the ability to synthesize IAA, but a substantial diversity of microorganisms also possess the ability to transform or degrade IAA (7), raising questions about the ecological significance of auxin metabolism and turnover in microorganisms.

An anaerobic auxin degradation pathway has been proposed in *Azoarcus evansii* and *Aromatoleum aromaticum* (8), and complete aerobic degradation of this auxin has been reported in *Bradyrhizobium* (9, 10); *Pseudomonas* (11); *Burkholderia*, *Rhodococcus*, and *Sphingomonas* (12); and *Acinetobacter* (13) species. Although two routes for aerobic IAA degradation were proposed some time ago in *Bradyrhizobium japonicum* (9, 10), with anthranilic acid as a key intermediate, genetic and additional biochemical aspects of aerobic IAA degradation have only been recently addressed (12, 14). Leveau and Gerards (12) were the first to describe genes related to IAA degradation in *Pseudomonas putida* 1290, which carries the *iacABCDEFGRHI* gene cluster, encoding conversion of IAA to catechol as intermediate (Fig. 1). After initial functional analysis of some *iac* genes in *P. putida* 1290, Scott et al. (14) proposed two putative intermediates based on the fact that the *iacA* gene product would start IAA degradation, hydroxylating IAA in position 3 of the indole ring, thus generating 2-hydroxyindole-3-acetic acid by migration of the hydroxyl group from indole ring position 3 to position 2 (Fig. 1A). They also suggested that the *iacE* gene product would be involved in the next step, transforming 2-hydroxyindole-3-acetic acid to 3-hydroxy-2-oxindole-3-acetic acid (dioxindole-3-acetic acid [DOAA]), which would be the substrate for the *iacC* gene function (Fig. 1A), in a rate-limiting step that also requires the *iacD* gene function, proposed as a subunit of the *iacC* gene product, based on sequence similarity analysis (14). In addition, catechol was identified as the end product of this IAA degradation pathway (Fig. 1A) (12, 14). More recently, the *iacR* gene from *Acinetobacter baumannii*, encoding a putative MarR-type transcriptional regulator, was reported to control *iac* gene repression in the absence of IAA (15). The roles of other *iac* genes remain unknown.

iac gene homologues are present in several *Proteobacteria* and *Actinobacteria* but with different gene organizations (12). The well-known plant-growth-promoting rhizo-

bacterium (PGPR) *Paraburkholderia* (formerly *Burkholderia* [16]) *phytofirmans* PsJN (17–19) possesses a cluster of *iac* genes related to those described in *P. putida* 1290 (Fig. 1B) (12) but with additional genes encoding putative regulatory, transport, and enzymatic functions. Remarkably, *P. phytofirmans* also synthesizes IAA (20) through at least two putative IAA biosynthesis routes (21), but additional studies are clearly required to understand IAA synthesis in this strain. Studies in *P. phytofirmans* PsJN indicate that production of the enzyme 1-aminocyclopropane-1-carboxylate deaminase, signaling via *N*-acylhomoserine lactones (quorum sensing), tryptophan-dependent IAA biosynthesis, and IAA degradation all play significant roles in plant colonization and plant growth promotion (19–22). Understanding the role of IAA in plant growth promotion in this and other bacteria is clearly precluded by the scarce knowledge on both the biochemical and genetic aspects of IAA degradation.

We reported here that *P. phytofirmans* PsJN mineralizes IAA using *iac* gene homologue-encoded functions. The role of some previously uncharacterized *iac* genes is also reported. IAA degradation by strain PsJN apparently uses some functionally redundant genes and other genes not previously reported in *P. putida* 1290, encoding transport and tautomerase superfamily enzymes. We also reported that, in contrast with *P. putida* and *A. baumannii*, where *iac* gene regulation is controlled by a MarR-type transcriptional repressor responding to the IAA molecule (14, 15), IAA degradation in *P. phytofirmans* is regulated by a two-component system and a LysR-type activator, which apparently respond to IAA in combination with DOAA, the previously proposed intermediate in strain 1290 (14).

RESULTS AND DISCUSSION

Genetic determinants involved in growth of *P. phytofirmans* PsJN on IAA. To evaluate mineralization of IAA by strain PsJN, growth tests were carried out in minimal medium cultures containing exogenously supplied auxin. Results showed that strain PsJN uses IAA as a sole carbon and energy source (Fig. 2). *P. phytofirmans* also utilized IAA as a sole nitrogen source, since it grows in a minimal medium with no added nitrogen sources (data not shown). Strain PsJN presented maximum specific growth rates (μ_{max}) (doubling times) of 0.21 $\pm$ 0.01 h^{-1} (3.24 $\pm$ 0.21 h) and 0.12 $\pm$ 0.01 h^{-1} (5.95 $\pm$ 0.16 h) with 2.5 and 5 mM IAA, respectively (Fig. 2). In contrast, strain PsJN exhibited μ_{max} (doubling times) of 0.42 $\pm$ 0.15 h^{-1} (1.83 $\pm$ 0.67 h) and 0.38 $\pm$ 0.17 h^{-1} (2.09 $\pm$ 0.78 h) with 2.5 and 5 mM benzoate (Bz), respectively (Fig. 2). Growth yields were estimated in 1.15 $\pm$ 0.19 and 1.89 $\pm$ 0.42 mg of cells/mmol of added carbon, for IAA and Bz, respectively.

Lag-phase values for growth on IAA, calculated according to the method of Baty et al. (23), were 8.26 $\pm$ 0.18 h and 18.95 $\pm$ 5.54 h in 2.5 mM and 5 mM IAA, respectively. In contrast, growth on Bz exhibited lag phases of 3.61 $\pm$ 1.54 h (2.5 mM Bz) and 4.09 $\pm$ 2.81 h (5 mM Bz) (Fig. 2). The lag phase of strain PsJN for growth on IAA is also longer than that of *P. putida* 1290 (12), which may be explained by a tightly controlled *iac* gene induction to avoid formation of higher levels of toxic intermediates. In this context, accumulation of catechol, a toxic intermediate preventing bacterial growth (24–26), was reported by Scott et al. (14) and also detected in this study (see below). Since the same concentrations of IAA (a 10-carbon-atom molecule) and Bz (a seven-carbon molecule) produce similar biomass yields (Fig. 2), with the two compounds sharing the six-carbon-molecule catechol as a key intermediate, it is also possible that IAA degradation could generate some dead-end metabolites or CO_2 as by-products, which are not utilized by cells.

Search of IAA degradation molecular determinants in the genome of strain PsJN allowed detection of *P. putida* 1290 *iac* gene homologues but with a different organization from that of strain 1290 (Fig. 1B) (12). Comparisons between *iac* homologues showed amino acid identities ranging from 38 to 62% (see Table S1 in the supplemental material). Only the *iacR* gene strain 1290 homologue, a transcriptional repressor belonging to the MarR family (14, 15), is absent in the strain PsJN genome. The strain PsJN *iac* gene sequences are adjacent to other genes, not found in *P. putida* 1290,

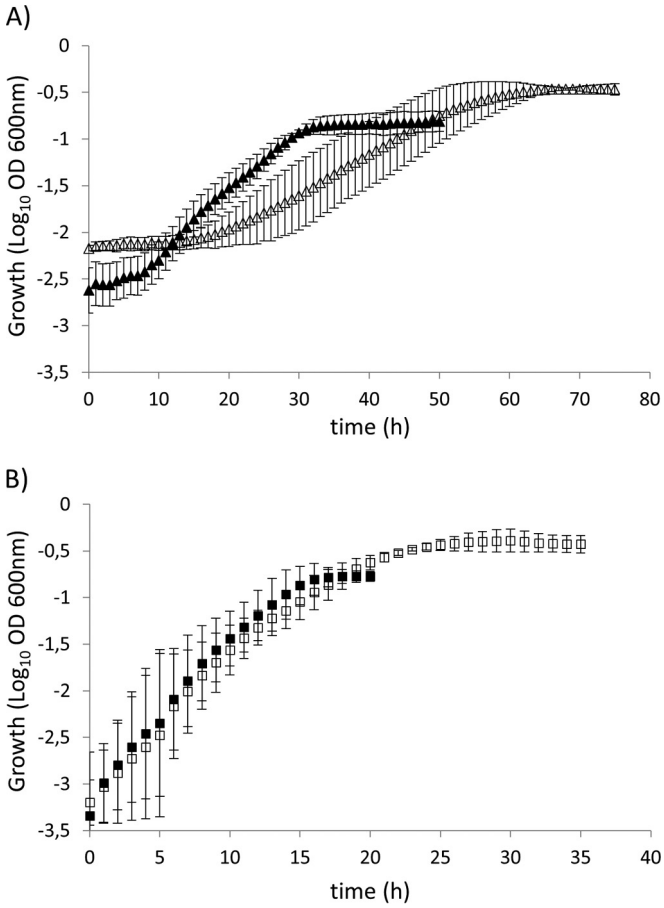

FIG 2 Growth of *Paraburkholderia phytofirmans* PsJN on indole-3-acetic acid (IAA) (A) or benzoate (Bz) (B) as the sole carbon and energy source. Symbols: closed squares, 2.5 mM Bz; open squares, 5 mM Bz; closed triangles, 2.5 mM IAA; open triangles, 5 mM IAA. Three biological replicates were performed for growth measurements. Error bars represent standard deviations of the means.

possibly playing regulatory and transport roles in IAA degradation (Fig. 1B). Among these are a histidine kinase signal transducer-encoding gene (named *iacS*) and a LuxR family protein receptor (*iacR1*), forming a putative two-component system; a transcriptional regulator belonging to the LysR family (*iacR2*); a transporter belonging to the major facilitator superfamily (*iacT1*); and a protein related to the tautomerase superfamily (*iacY*) (see Table S2 in the supplemental material).

To test if these *iac* genes are involved in IAA degradation, the corresponding strain PsJN mutants were generated and growth tests were performed with IAA as a sole carbon and energy source. With the exceptions of the *iacG* gene, the putative regulatory *iacS* gene, the putative transporter *iacT1* gene, and the *iacY* gene, all other *iac* genes (*iacA*, *-B*, *-C*, *-D*, *-E*, *-F*, *-H*, and *-I*) were required for growth of strain PsJN on IAA, as no growth of the corresponding mutant strains was detected, even if cells were cultured for 7 days (see Table S3 in the supplemental material). It was previously reported in *P. putida* 1290 that the *iacH* gene was not essential for IAA degradation (12), suggesting that insertional mutation (single crossover employing a suicide plasmid) could cause polar effects in strain PsJN over genes that would belong to the same transcriptional unit, i.e., *iacABIHE* and *iacCDYT1* genes (Fig. 1B; see Fig. S1 in the supplemental material). In order to evaluate this possibility, the *iacH* mutant strain was complemented with the *iacH* gene or the contiguous downstream *iacE* gene. IAA growth was recovered only in the *iacE*-complemented strain (Table S3), strongly indicating that interruption of the *iacH* gene caused a polar effect over the *iacE* gene

and supporting the idea that *iacH* was not essential for IAA degradation in strain PsJN, at least under the tested conditions.

To verify if other *iac* genes that may be organized as an operon (*iacA*, *iacB*, *iacC*, and *iacI* [Fig. 1B; Fig. S1]) are key in the IAA degradation pathway, mutant strains of these genes were supplemented with plasmid constructions containing all other *iac* genes (*iacABIHECDGF*), with or without the respective interrupted gene (plasmids in Table 1). Growth on IAA was recovered only in the presence of the corresponding interrupted genes, showing that *iacA*, *iacB*, *iacC*, and *iacI* genes are essential in the IAA degradation pathway (Table S3). In turn, growth on IAA of the *iacG* and *iacS* gene mutants was only partially diminished (Table S3), suggesting that their functions were in part replaced by other genes carried in the genome of strain PsJN. Remarkably, *iacA*, *iacG*, and *iacT1* genes possess homologues in the *P. phytofirmans* genome, referred to as *iacA2* (65% amino acid identity with *iacA*), *iacG2* (63% amino acid identity with *iacG*), and *iacT2* (51% amino acid identity with *iacT1*), which are clustered together (Fig. 1B). However, single mutants of these genes have no influence on growth of IAA, at least under the tested conditions (Table S3).

P. putida 1290 mutants for *ortho*-ring cleavage catechol degradation turn IAA growth test plates brown (12), and cell extracts of *P. putida* 1290 grown on IAA show elevated levels of catechol 1,2-dioxygenase activity (11), suggesting that IAA catabolism in strain 1290 produces catechol as intermediate, a possibility that was later confirmed by Scott et al. (14) through gas chromatography-mass spectroscopy analysis. The genome of *P. phytofirmans* PsJN has a putative *ortho*-ring cleavage catechol pathway gene cluster, encoding catechol 1,2-dioxygenase (*catA*), muconate cycloisomerase (*catB*), and muconolactone isomerase (*catC*), located adjacent to the *iac* gene cluster (Fig. 1B; Table S2), presumably involved in the degradation of catechol via *cis*,*cis*-muconic acid (27). A *P. phytofirmans* PsJN *catA* mutant was generated to evaluate if this putative catechol 1,2-dioxygenase effectively contributes to IAA degradation. The strain PsJN *catA* mutant turned fructose plates brown when supplemented with IAA (see Fig. S2 in the supplemental material), suggesting catechol accumulation and polymerization (24). This *catA* mutant was completely unable to grow on IAA (Table S3), strongly indicating its involvement in IAA degradation. A second putative catechol 1,2-dioxygenase-encoding gene (*catA2*) is also present in the strain PsJN genome, clustered with Bz 1,2-dioxygenase genes (Table S2) and therefore putatively involved in Bz catabolism. The *catA2* gene seems to not be directly participating in IAA degradation because the *catA* gene mutant completely lost this ability. As expected, the *catA* mutant still grows on Bz (Table S3). When this *catA* mutant was exposed to 2.5 mM IAA plus 0.25 mM Bz (as an inducer of the additional CatA2 catechol 1,2-dioxygenase gene), this mutant recovered the ability to grow on IAA but turned the growth medium brown (data not shown), demonstrating that catechol accumulated by *iac* genes activity is partially metabolized by CatA2.

***P. phytofirmans* PsJN IAA degradation pathway.** Scott et al. (14) reported that the *iacA*, *iacE*, and *iacC* gene products are involved in consecutive steps of the IAA degradation pathway in *P. putida* 1290, whereas the roles of other *iac* genes remained unclear. To advance the elucidation of biochemical steps encoded by all strain PsJN *iac* genes in IAA degradation, several *iac* gene sets were cloned into the strain *Cupriavidus pinatubonensis* JMP134, which is heterologous but belongs to the same family (*Burkholderiaceae*). This strain, taxonomically and metabolically related to *P. phytofirmans* PsJN (28–30), lacks *iac* gene sequence homologues and is unable to use IAA as a sole carbon and energy source (Table S3), which allow its use as an appropriate heterologous host for *iac* genes. A strain JMP134 derivative carrying the *P. phytofirmans iacABIHECDGF* genes (named strain JMP134*iac*1) turned fructose growth test plates brown when supplemented with IAA, suggesting IAA removal and catechol accumulation comparable to those of the strain PsJN *catA* mutant (Fig. S2). As strain JMP134 has functional *catA* genes, most likely they were not induced by catechol produced from IAA under the tested conditions. Resting cell assays of strain JMP134*iac*1 dem-

onstrated IAA consumption and transient catechol accumulation in high-performance liquid chromatography UV detection (HPLC-UV) profiles (see Fig. S3 in the supplemental material). Nevertheless, an additional intermediate was detected in these assays (initially designated compound 1 [Fig. S3]) that was not removed even after 43 h of incubation. In order to identify compound 1 as an intermediate during IAA degradation (see below), the accumulated metabolite was extracted from the JMP134*iac*1 supernatant organic phase at low pH using ethyl acetate, allowing purification of a single compound as detected by thin-layer chromatography (data not shown). Determination of the relative mass formula of the purified metabolite by mass spectrometry indicated that *m/z* of the molecular ion peak was 207.20, while infrared analysis showed that the molecule has -OH and CO- functional groups (infrared [IR] [KBr] cm^{-1}, 3,313 [OH]; 1,702 [CO]). Analysis by ^{1}H and ^{13}C nuclear magnetic resonance (NMR) spectroscopy suggested that purified compound 1 is 2-(3-hydroxy-2-oxoindolin-3-yl)acetic acid (also named dioxindole-3-acetic acid) (see Table S4 in the supplemental material) comparable to that proposed by Scott et al. (14) (Fig. 1A). The molecular formula of this compound is $C_{10}H_9NO_4$ with a calculated mass of 207.18 g/mol, which is quite close to the relative mass formula indicated above, strongly suggesting that the compound proposed by Scott et al. (14) is an IAA degradation product.

When strain PsJN IAA-grown cells were exposed to the supernatant containing compound 1, i.e., DOAA, fast and complete removal of this compound was observed (see Fig. S4 in the supplemental material), suggesting that strain JMP134*iac*1 lacks a function related to DOAA metabolism that is present in *P. phytofirmans*. A possible candidate for the missing function is the *iacT1* gene (Fig. 1B; Table S2), encoding a putative transporter that could allow internalization of this intermediate to restart metabolism. Another possible candidate is the *iacY* gene (Table S2), located apparently in the same transcriptional unit next to the *iacT1* gene (Fig. 1B; Fig. S1), encoding a protein belonging to a tautomerase superfamily. To test these possibilities, both the *iacY* and *iacT1* gene sequences were cloned and introduced into the JMP134*iac*1 derivative accumulating DOAA. Results showed that only when the two genes were simultaneously present in the JMP134*iac*1 derivative was DOAA completely removed after 24 h of incubation (see Fig. S5 in the supplemental material). Remarkably, despite the fact that *iacT1* and *iacY* mutant strains are able to use IAA as a sole carbon and energy source (Table S3), DOAA growth tests specifically performed with these mutants showed that they were unable to grow on DOAA, unlike the wild-type strain, indicating that the *iacT1* and *iacY* genes are a functional part of the *P. phytofirmans iac* gene cluster, as their gene products play a role in DOAA removal in the biochemical route of IAA degradation. Database searches predicted that the *iacT1* gene, and also the *iacT2* gene found clustered with the *iacA2* and *iacG2* genes (Fig. 1B), belong to the major facilitator superfamily of transporters, which are single-polypeptide secondary carriers capable of transporting small solutes in response to chemiosmotic ion gradients (31), and specifically belong to the metabolite-H^+ symporter family related to the shikimate transporter encoded by the *shiA* gene of *Escherichia coli* (~40% amino acid identity) (32). These data suggest that the *iacT1*-encoded product is a DOAA transporter. In turn, the *iacY* gene would encode a protein belonging to a tautomerase superfamily characterized by catalytic promiscuity with a key catalytic amino-terminal proline (33). The *iacY*-encoded product is a long monomer related to the enzyme 4-oxalocrotonate tautomerase that catalyzes ketoenol tautomerization of 2-hydroxy-2,4-hexadienedioate (2-hydroxymuconate) to 2-keto-3-hexenedioate, which is part of the catabolic *meta*-cleavage pathway for aromatic compounds such as toluene or its derivatives (34). In the case of the *iacY*-encoded product, its role in DOAA metabolism remains elusive.

A series of additional incomplete JMP134*iac*1 derivatives were incubated with IAA, and the incubation supernatants were analyzed by HPLC-UV at different times. As expected, only the JMP134 strain carrying all *iac* genes except *iacA* (JMP134*iac*1ΔA) was unable to remove IAA (see Fig. S6 in the supplemental material), demonstrating that the *iacA* gene encodes the first step in the IAA degradation pathway of *P. phytofirmans*, in agreement with the findings reported by Lin et al. (13) and Scott et al. (14) in *A.*

baumannii ATCC 19606 and *P. putida* 1290, respectively. Amino acid sequence analysis predicted that IacA would belong to the acyl coenzyme A (acyl-CoA) dehydrogenase flavoprotein family (13, 35). Conversion of indole into indigo (through indoxyl production) was demonstrated for the *A. baumannii* ATCC 19606 *iacA* gene product, whose reaction was absolutely dependent on NADH and flavin adenine dinucleotide (FAD) (13), supporting its classification as a flavoprotein. Moreover, Scott et al. (14) proposed that the IacA protein hydroxylates IAA to 2-hydroxyindole-3-acetic acid (Fig. 1A), indicating that IacA protein would have an IAA hydroxylase activity. Remarkably, the strain JMP134*iac*1ΔG derivative removed IAA significantly slower than strain JMP134*iac*1, as more than half of the initial IAA was still present after 10 h of incubation (Fig. S6). These results suggested that the *iacA* and the uncharacterized *iacG* gene products might work together and participate in the initial attack on IAA. To test this assumption, the *iacA* gene sequence was cloned in *C. pinatubonensis* JMP134, alone or in combination with the *iacG* gene, generating strain JMP134-*iacA* or -*iacAG* derivatives, respectively. Resting cells of strain JMP134-*iacA* exposed to IAA were unable to remove IAA (data not shown), whereas strain JMP134-*iacAG* cells quickly transformed IAA into different compounds (compounds X and Y [see Fig. S7A in the supplemental material]), supporting their role in the initial attack of IAA. Remarkably, the strain JMP134 derivative harboring redundant *iacA2G2* genes (Fig. 1B), but not the JMP134 derivative carrying only the *iacA2* gene, was also able to transform IAA to compounds X and Y (data not shown), suggesting that additional copies of *iacAG* are effectively functional. Cell extracts of derivatives JMP134-*iacAG* and -*iacA2G2* confirmed consumption of NADH during IAA transformation, showing that enzymatic activity related to NADH conversion to NAD^+ of the strain containing *iacA2G2* was lower than that of the strain containing *iacAG* (data not shown). Interestingly, strain JMP134 derivatives carrying the *iacAG* genes but not the *iacA2G2* genes have the capacity to transform indole into the blue insoluble compound named indigo (data not shown).

The role of the *iacG* gene does not seem to be essential for IAA degradation in *P. phytofirmans* because the *iacG* gene has at least two additional equivalents in the genome of strain PsJN (Table S1), one of them being functional (*iacG2*). Also, the IacG protein may have an accessory role, which is supported by the fact that the *iacG* gene sequence has the best hit (56% of amino acid identity) with the 4-hydroxyphenylacetate (4-HPA) 3-monooxygenase reductase component (*hpaC* gene) of *E. coli* (36), which is able to reduce FAD to $FADH_2$, to dissociate from the enzyme, and later to be captured by the 4-HPA 3-monooxygenase (HpaB) to hydroxylate 4-HPA. Therefore, direct interaction between HpaB and HpaC is not critical, and thus, theoretically, any flavin reductase present in the host cell would replace HpaC (36). Correspondingly, IacG would provide reduced flavins to IacA in the first step of the IAA degradation pathway in *P. phytofirmans* in an NADH-dependent step (Fig. 3A).

Additional experiments indicated that the strain JMP134*iac*1ΔE derivative completely removed IAA from the medium after 10 h, accumulating compounds X and Y (Fig. S6), similarly to the strain JMP134-*iacAG* derivative (Fig. S7A). Scott et al. (14) reported that the *P. putida iacE* gene product participates in the second step of the IAA pathway (Fig. 1A), encoding an enzyme involved in the formation of 3-hydroxy-2-oxindole-3-acetic acid (DOAA) from 2-hydroxyindole-3-acetic acid. Sequence analysis predicted that the *iacE* gene product of strain PsJN would be a classical member of the short-chain dehydrogenase/reductase (SDR) family, characterized by a Rossmann-fold scaffold, typically about 250 residues long, with specific cofactor (TGxxxGxG) and active site (YxxxK) sequence motifs and a reaction spectrum comprising the NAD(P)(H)-dependent oxidoreduction of hydroxy/keto groups (37). In turn, the strain JMP134*iac*1ΔB derivative exposed to IAA resulted in production of compounds X and Y but also detectable amounts of DOAA (Fig. S6), suggesting that IacE and IacB work together. To test this possibility, the ability of the strain JMP134-*iacE*, -*iacB*, or -*iacEB* derivatives to transform supernatants of strain JMP134-*iacAG* exposed to IAA, containing intermediate compounds X and Y (Fig. S7A), was determined. The strain JMP134-*iacE* and -*iacEB* derivatives transformed supernatants produced by the

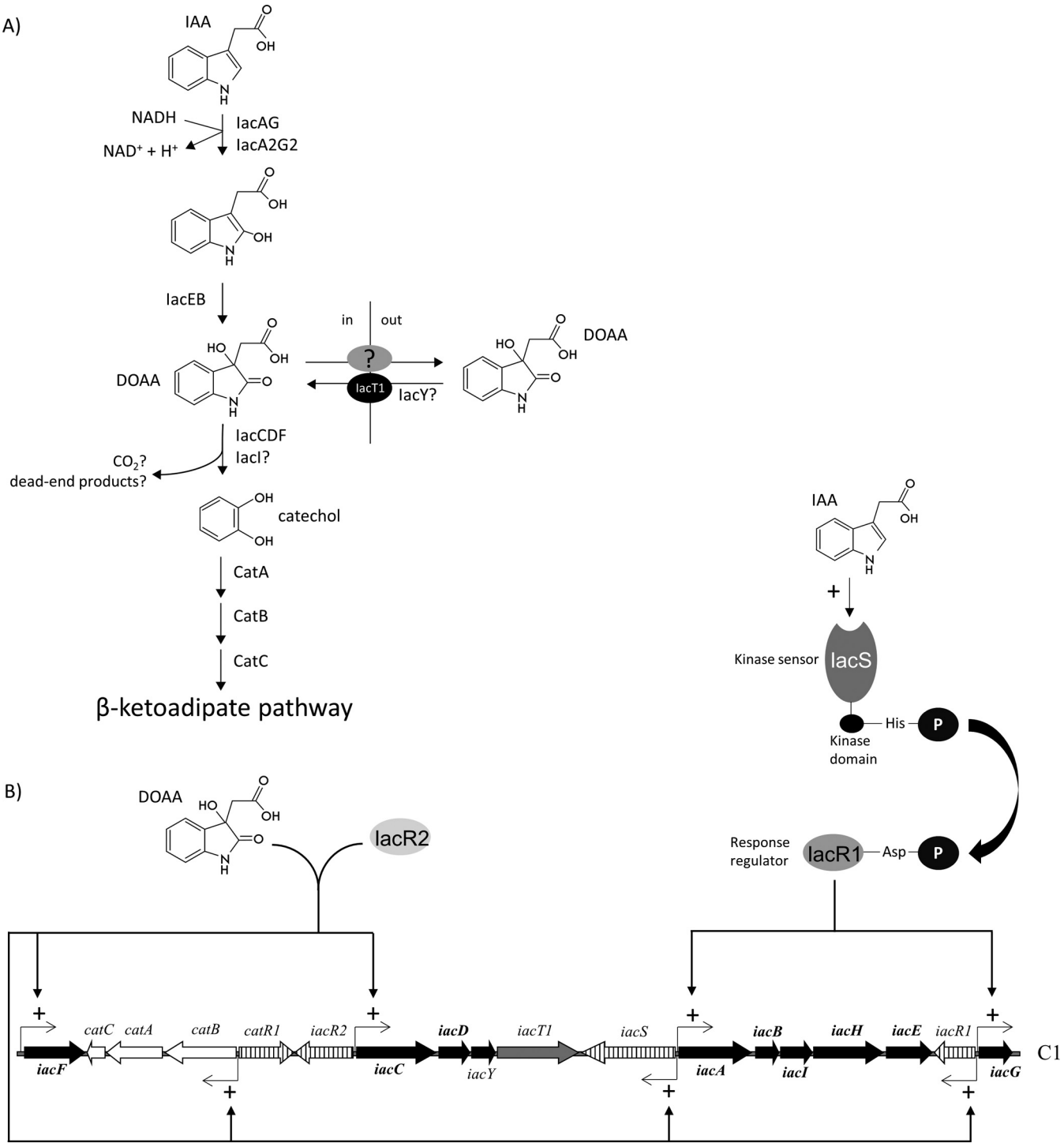

FIG 3 Putative roles of *Paraburkholderia phytofirmans* PsJN *iac* genes (A) and their regulation in auxin phytohormone indole-3-acetic acid (IAA) degradation (B). DOAA, dioxindole-3-acetic acid; in, intracellular space; out, extracellular space; ?, not known.

strain JMP134-*iacAG* derivative, generating DOAA, although the strain JMP134-*iacEB* derivative produced significantly larger amounts of DOAA (Fig. S7B), than the strain JMP134-*iacE* derivative (data not shown). These results strongly suggest that IacB may be an auxiliary or accessory protein of the IacE protein, as the strain JMP134-*iacB* derivative did not produce DOAA (data not shown). The *P. phytofirmans iacB* gene sequence analysis shows no conserved domains, and no function could be predicted from its primary structure, although a role of IacB as an IacE auxiliary or accessory protein cannot be dismissed, since

production of DOAA would require a hydroxylation step (Fig. 1A) (19) not catalyzed by a classical dehydrogenase activity (37). Then, a second hydroxylation step in the IAA degradation pathway would be a result of the IacEB protein activity (Fig. 3A). However, a possible participation of *iacAG* gene products in a second hydroxylation on the IAA molecule cannot be discarded, since strain JMP134-*iacAG* exposed to IAA generated several compounds (Fig. S7A), which could correspond to interchangeable forms of the hydroxylated IAA, and therefore, IacEB may perform a subsequent hydroxy/keto reduction step to produce DOAA.

The strain JMP134*iac*1ΔCD, -*iac*1ΔF, and -*iac*1ΔI derivatives completely removed IAA and accumulated large amounts of DOAA (Fig. S6). When the strain JMP134-*iacCDFI* derivative was exposed to a supernatant containing only DOAA, this compound remained intact (data not shown), which clearly suggested that the *iacT1* and *iacY* gene products (see above) are required before the participation of the *iacCDFI* gene products. To test this option, the strain JMP134-*iacC*, -*iacCD*, -*iacCDF*, or -*iacCDFI* derivatives additionally harboring *iacY* and *iacT1* genes were exposed to supernatants containing DOAA. Results showed that strain JMP134-*iacC* and -*iacCD* derivatives were unable to transform DOAA (data not shown), whereas the strain JMP134-*iacCDF* derivative converted DOAA to catechol (Fig. S7C). It is worth noting that the strain JMP134-*iacCDFI* derivative transformed DOAA faster than the strain JMP134-*iacCDF* derivative, with no accumulation of catechol (data not shown). Sequence analysis showed that the *iacC* gene product of *P. phytofirmans* PsJN belongs to the Rieske nonheme iron oxygenase family (38, 39), whereas the *iacD* gene product belongs to the beta subunit of ring hydroxylating dioxygenases, which has a structure similar to that of NTF-2 and scytalone dehydratase (40, 41). Rieske nonheme iron oxygenase systems use nonheme Fe(II) to catalyze addition of hydroxyl groups to the aromatic ring, an initial step in oxidative degradation of aromatic compounds (38, 39), employing an electron transport chain to use NAD(P)H and activate molecular oxygen (38). Some oxygenase components contain a beta subunit, but with a purely structural function, although some reports suggest that they can influence substrate binding in some oxygenases (42). Then, alpha subunits are the catalytic components, carrying an N-terminal domain which binds a Rieske-like [2Fe-2S] cluster that accepts electrons from a reductase or ferredoxin and passes them to a C-terminal catalytic domain, which binds the nonheme Fe(II) for catalysis (38). Rieske nonheme iron oxygenase systems are constituted by additional components involved in transfer of an electron from NAD(P)H to O_2: a reductase, a ferredoxin (only in three-component systems), and the previously indicated oxygenases (with oligomer α_3 or $\alpha_3\beta_3$) (38, 39). Sequence analysis of the *iacF* gene product revealed that it belongs to the ferredoxin-NADP reductase family (43), which contains an FAD or flavin mononucleotide (FMN) binding domain, an NADH binding domain, and a plant-type [2Fe-2S] cluster domain, catalyzing transfer of reducing equivalents between the $NADP^+$/NADPH pair and the oxygenase component (38, 43). Consequently, the *iacF* gene product would be the reductase component of an aromatic ring hydroxylating dioxygenase, with the *iacC* and *iacD* genes as the oxygenase components (alpha and beta subunits, respectively). This assumption was supported by catechol production from DOAA in the strain JMP134 derivative carrying *iacCDF* genes plus *iacY* and *iacT1* genes (Fig. S7C). Remarkably, the absence of the *iacI* gene in the strain JMP134*iac*1ΔI derivative produced an accumulation of DOAA (similar to the effect of the absence of the *iacCD* and *iacF* genes), and the strain PsJN *iacI* mutant was unable to use DOAA as sole carbon and energy source, suggesting a role in a biochemical step downstream from the reaction carried out by the *iacY* and *iacT1* gene products. Amino acid sequence analysis of IacI showed similarity with members of the SnoaL-4 superfamily, which is a family of proteins that shares the SnoaL fold, mainly represented by polyketide cyclases catalyzing ring closure steps in polyketide antibiotic synthesis (44). The presence of the *iacI* gene in the strain JMP134 *iacCDFYT1* gene derivative accelerated removal of DOAA. Thus, it is likely that IacI participates in the same or in a later IAA degradation step catalyzed by IacCDF (Fig. 3A).

Finally, the strain JMP134*iac*1ΔH derivative fully removed IAA and accumulated DOAA and catechol (data not shown), analogously to strain JMP134*iac*1, corroborating

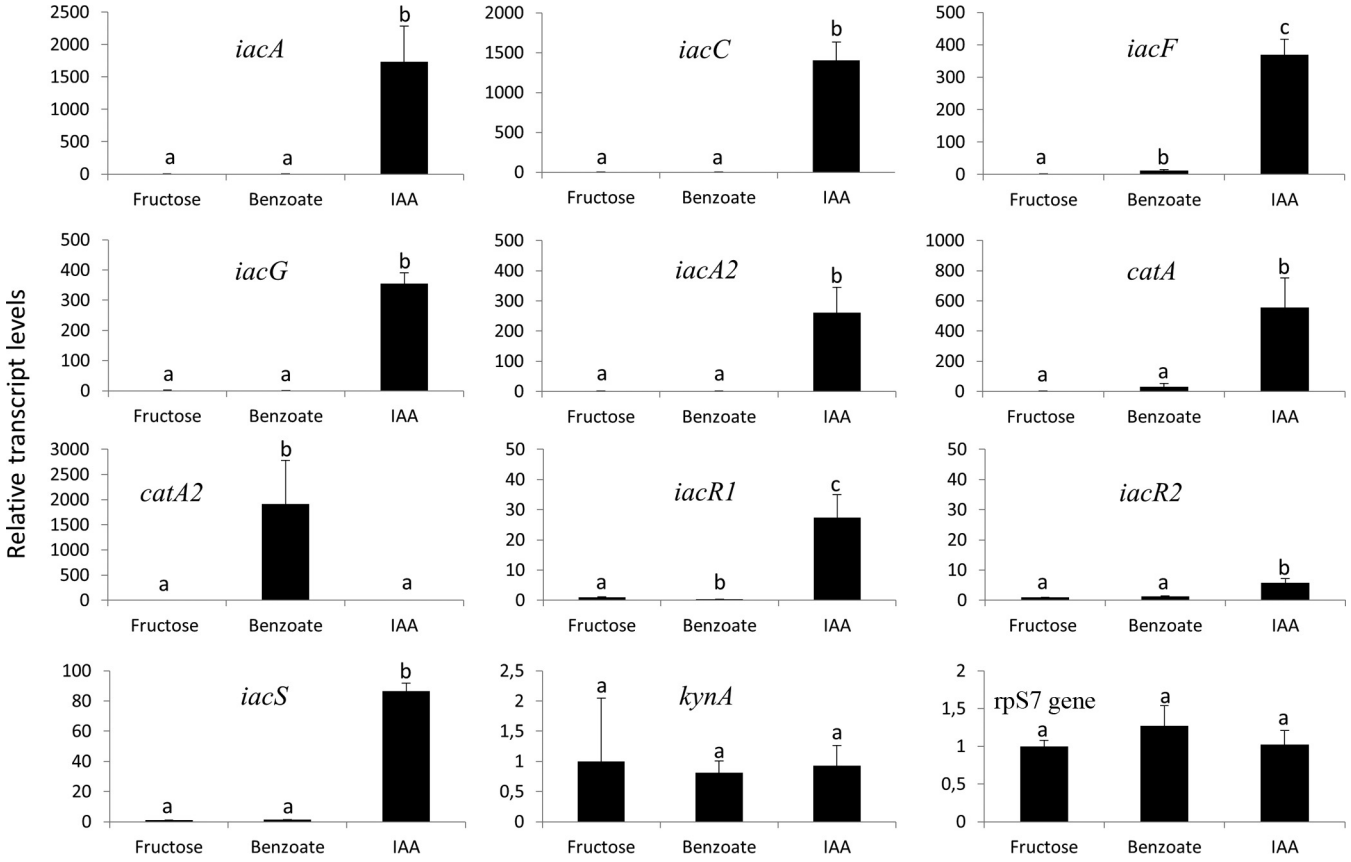

FIG 4 Transcript levels of *iac* and *cat* genes from *Paraburkholderia phytofirmans* cells exposed to indole-3-acetic acid (IAA). Real-time PCR analysis of *iac* and *cat* genes in cells grown on fructose, benzoate, or IAA as a sole carbon and energy source. It should be noted that transcript levels of the ribosomal protein S7 (rpS7) and tryptophan dioxygenase (*kynA*) genes, used as expression controls, remained unchanged under these conditions. Transcript levels were normalized to the average value of the transcript levels in fructose treatment. 16S rRNA was used as a reference gene (internal control). Note different scales. All experiments were performed in three biological replicates. Error bars represent standard deviations. Different letters indicate statistically significant differences between treatments (one-way analysis of variance, $P < 0.05$; Tukey's test, $P < 0.05$).

that the *iacH* gene-encoded product was not involved in IAA transformation to catechol under the tested conditions, similar to that reported in *P. putida* 1290 (12). Sequence analysis indicated that the *iacH* gene product of *P. putida* was related to amidases/amidohydrolases (12), analogous to that found for the strain PsJN homologue sequence. Auxin storage in plants includes conjugation to form IAA-amides, in which IAA is ligated to amino acids such as Ala, Asp, Phe, or Trp (45). Assays with a strain JMP134 derivative overexpressing the *iacH* gene dismissed the use of indole-3-acetamide or indole-3-acetonitrile (data not shown), although further research is needed to test a possible role of the *iacH* gene product in IAA-amide conjugate metabolism.

Analysis of *iac* and *cat* gene expression in *P. phytofirmans* PsJN. To evaluate *iac* gene expression, a quantitative real-time PCR analysis of RNA extracted from mid-log-phase cells of *P. phytofirmans* PsJN growing on IAA, Bz, or fructose as a sole carbon and energy source was performed. Results showed that transcript levels of the *iacA*, *iacC*, *iacF*, and *iacG* genes in IAA-grown cells were at least 2 orders of magnitude higher than those in cells growing on fructose or Bz (Fig. 4). Transcript levels of the redundant *iacA2* gene were also increased in IAA-grown cells, suggesting a functional role in IAA degradation. Remarkably, transcript levels of the *iacS* and *iacR1* regulatory genes were also increased (approximately 50 times) in IAA-grown cells, whereas the *iacR2* transcript levels increased only five times in comparison with cells growing without IAA (Fig. 4). Moreover, *catA* transcript levels in IAA-grown cells were about 500 times higher than those in fructose- or Bz-grown cells, indicating that this catechol 1,2-dioxygenase is strongly induced during growth on IAA. In contrast, *catA2* transcript levels were not

increased in IAA-grown cells but they were significantly induced in Bz-grown cells (Fig. 4), supporting the idea that the *catA2* gene does not participate in auxin metabolism, as IAA is unable to induce this putative catechol 1,2-dioxygenase-encoding gene.

Additional analysis of the *iac-cat* gene organization of *P. phytofirmans* PsJN showed the presence of putative *iacABIHE*, *iacCDYT*, *iacF*, *iacG*, and *catBAC* transcriptional units (Fig. 1B; Fig. S1) and made it interesting to analyze the promoter activity profile of IAA degradation genes. β-Galactosidase transcriptional fusion assays with putative promoters of these transcriptional units were performed. Results showed that all *iac* gene promoters tested, including the *cat* gene promoter, were more active in the presence of the mixture of IAA and supernatant containing DOAA or compounds X and Y as inducers than in the presence of IAA or the supernatant containing DOAA or compounds X and Y alone (Fig. 5A), suggesting a coordinated and presumably complex promoter regulation of *iac*/*cat* gene expression. Additional tests of the *iac* promoter activities were performed with *P. phytofirmans* regulatory mutants containing mutations in the *iacS*, *iacR1*, and *iacR2* genes, exposed to mixtures of IAA and supernatant containing DOAA. Results showed that the *iacC*, *iacF*, and *catB* gene promoters were induced in the *P. phytofirmans iacS* or *iacR1* gene mutants (Fig. 5B) and were not induced in the *P. phytofirmans iacR2* gene mutant showing that *iacC*, *iacF*, and *catB* gene promoters are controlled by an *iacR2*-encoded regulator or another regulator controlled by IacR2 levels. Conversely, mixtures of IAA and supernatant containing DOAA did not induce the *iacA* and *iacG* gene promoters in the regulator mutant strains (Fig. 5B), indicating that these three *iac* regulators are involved in their control. Because *iacR2*-encoded regulators apparently handle all *iac*/*cat* promoters, quantitative real-time PCR analysis of RNA extracted from cells of the wild type and the *iacR2* mutant growing on fructose and induced with IAA-DOAA mixtures was accomplished to find out if the *iacR1* and *iacS* genes are controlled by IacR2. Results showed that cells with a background lacking the *iacR2* gene were unable to induce *iacR1* and *iacS* genes (see Fig. S8 in the supplemental material), demonstrating that transcription of both regulators is controlled by IacR2.

Compared with *P. putida* 1290, where the *iac* gene cluster includes only a transcriptional repressor belonging to the MarR family, named *iacR* (14, 15), which is absent in the genome of *P. phytofirman*s PsJN, the regulation of IAA catabolism in strain PsJN is far more complex: a histidine kinase signal transducer and a LuxR family protein receptor (a putative two-component system), *iacS* and *iacR1*, respectively, and a LysR-type transcriptional regulator (LTTR), *iacR2* (Fig. 1B). Only a few bacterial two-component systems involved in degradation of aromatic compounds have been characterized to date; they are related to toluene, biphenyl, and styrene degradation in *Pseudomonas*, *Thauera*, *Azoarcus*, and *Rhodococcus* strains (46–50). On the other hand, the LTTR family is a well-characterized group of transcriptional regulators, highly conserved and ubiquitous among bacteria (51), which have been involved in control of metabolism, cell division, quorum sensing, virulence, motility, and nitrogen fixation, among others (51–54). A larger subgroup of LTTRs is associated with degradation of aromatic compounds, in which regulators CatM and BenM of Bz catabolism are quite well studied (55, 56). It is reported here that the *iacR1* and *iacR2* genes are essential for *P. phytofirmans* IAA catabolism, whereas the lack of the *iacS* gene decreased catabolism of IAA. Based on their location in the *iac* gene cluster (Fig. 1B) and the promoter activities of the corresponding mutant strains reported here (Fig. 5B), it is quite possible that the *iacS/iacR1* gene product pair is a two-component system, with the *iacS* gene product sensing added IAA, autophosphorylating, and then phosphorylating *iacR1*, which positively interacts with the *iacA* and *iacG* gene promoters (Fig. 5B). Interestingly, Leveau and Gerards (12) found that mutants in a gene with amino acid similarity to the kinase sensor of the two-component system CbrAB of *Pseudomonas aeruginosa* PAO1 are unable to use IAA. CbrAB-inactivated strain PAO1 derivatives are also unable to grow on several N-substrates, suggesting that CbrAB controls expression of catabolic pathways in response to changing intracellular C/N ratios (57). The results reported here allow us to propose that the *iacR2* gene product is a classical LysR transcriptional

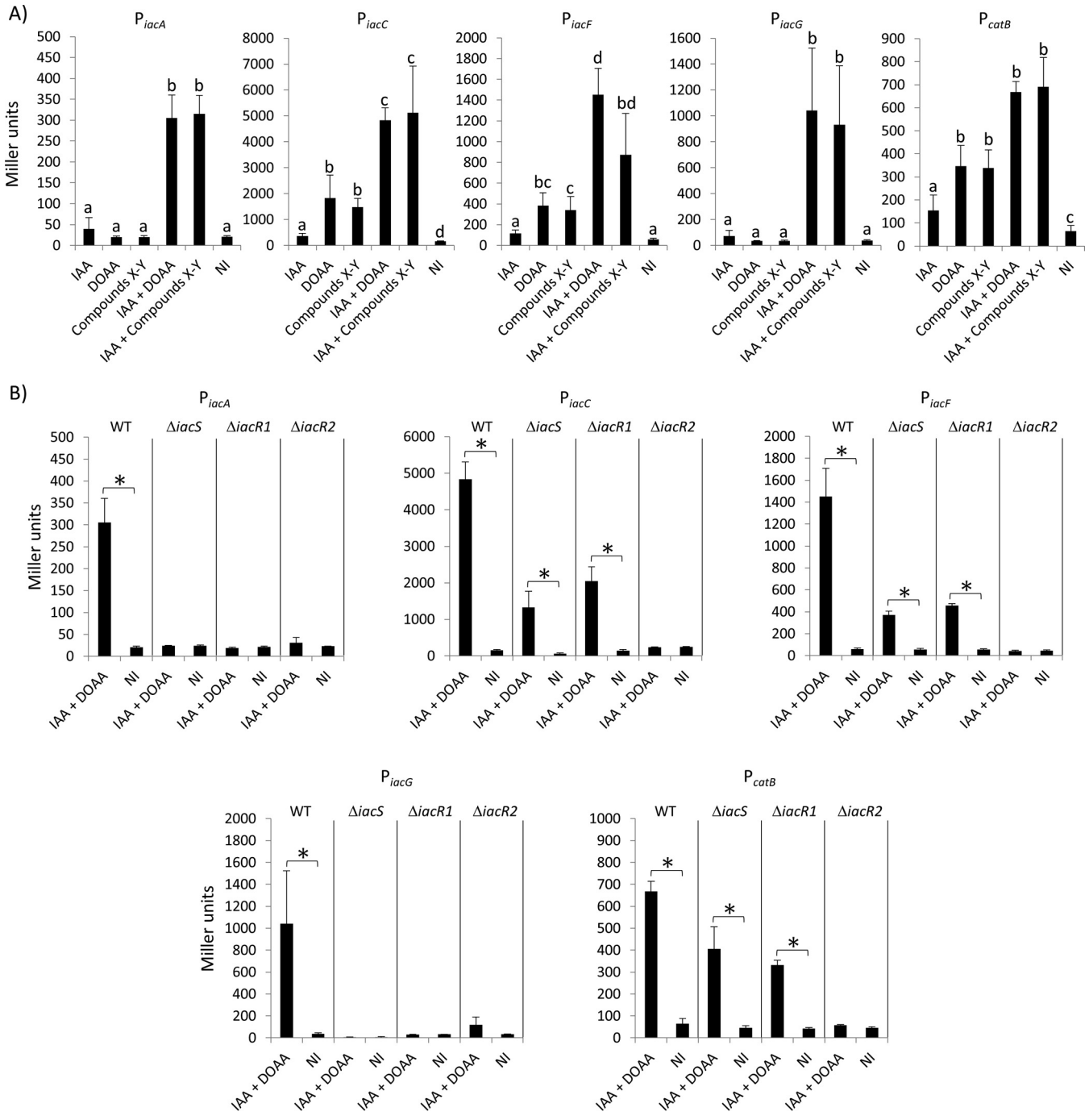

FIG 5 Induction of *iac* and *cat* promoter activities from *Paraburkholderia phytofirmans* PsJN and derivative mutants by mixtures of indole-3-acetic acid (IAA) and dioxindole-3-acetic acid (DOAA) or compounds X and Y. β-Galactosidase activity levels obtained from transcriptional fusions of *iacA*, *iacC*, *iacF*, *iacG*, and *catB* genes exposed to IAA, DOAA, compounds X and Y or mixtures of IAA plus DOAA or compounds X and Y in the wild-type strain (A) and in the mutant derivatives defective in *iacS*, *iacR1*, or *iacR2* (B). Compounds X and Y or DOAA was prepared using 4-fold-diluted supernatants of strain JMP134-*iacAG* or JMP134*iac*1 resting cells previously exposed to 1 mM IAA as the only carbon source for 2 h, respectively. Error bars indicate the standard deviations. WT, wild type; NI, noninduced. Different letters and asterisks indicate statistically significant differences between treatments (one-way analysis of variance, $P < 0.05$; Tukey's test, $P < 0.05$; Student's *t* test, $P < 0.05$).

regulator using DOAA generated by the *iacEB*-encoded products as a coinducer, thus inducing transcription of *iacC*, *iacF*, and *catB* genes (Fig. 4 and 5B). This system would also control transcription of *iacR1* and *iacS* genes. The latter possibility is based on the fact that these genes showed an increased expression (~50 times in comparison to the control) with IAA as an inducer, whereas the *iacR2* gene exhibited a much lower

induction level increase (Fig. 4), and that the *P. phytofirmans iacR2* mutant is unable to induce any *iac* promoter and to produce *iacS*/*iacR1* transcripts in the presence of the tested inducers (Fig. 5B; Fig. S8). In addition, IAA degradation *cat* genes in strain PsJN is associated with a CatR-like regulator (Fig. 1B), similar to CatM and BenM of Bz catabolism (55, 56). However, participation by this regulator remains unclear because strain PsJN *cat* genes are regulated by IacR2 (Fig. 5B). Additional research is required to find out if *catR*/*iacR2*-encoded regulators are able to interact.

Outlook. The IAA degradation *iac* genes reported in *P. putida* 1290 are present in several bacteria belonging to *Alphaproteobacteria*, *Betaproteobacteria*, *Gammaproteobacteria*, and *Actinobacteria* (12). The beneficial plant-related bacterium *P. phytofirmans* PsJN also harbors *iac* genes but with a different gene organization, including additional transport, enzymatic, and regulatory genes. Results reported here showed biochemical steps in which *iac* genes with unknown functions would be participating (Fig. 5A) and also showed two additional uncharacterized genes related to major facilitator and tautomerase superfamilies involved in removal of the DOAA intermediate (Fig. 1A and 3A). Additionally, *iac* genes encoding the initial attack on the IAA molecule would be redundant, as an *iac*-related second gene cluster is also present in *P. phytofirmans*. Apparent redundancy, indicated by results reported here for the *iacA2* and *iacG2* genes, as the *iacA2* gene was induced in *P. phytofirmans* cells grown on IAA (Fig. 4), and indicated by the fact that the *iacA2G2* genes expressed in combination enable the removal of IAA, may be utilized to extend the spectrum of plant-derived IAA-like molecules. Such a possibility would be supported by a different specificity of *iacAG* gene products, as the *iacA2G2* gene products do not transform indole to indigo under the tested conditions, and the *iacA2G2*-encoded product has a lower enzymatic activity against IAA than does IacAG (data not shown). Furthermore, this apparent functional gene redundancy would provide a selective metabolic advantage associated with previously reported IAA toxicity over plant and animal membranes (58). For instance, two copies of (chloro)catechol 1,2-dioxygenase avoid accumulation of toxic (chloro) catechol intermediates (25, 26) or dead-end metabolite production, as in strains *C. pinatubonensis* JMP134 and *Cupriavidus metallidurans* CH34, which harbor two copies of phenol monooxygenases: one copy is associated with catechol 1,2-dioxygenase and the other with catechol 2,3-dioxygenase (30), depending on whether the provided substrate (e.g., phenol or methylphenols) is channeling through *ortho* (catechol 1,2-dioxygenase) or *meta* (catechol 2,3-dioxygenase) cleavage (59).

The *iac* gene regulation in *P. phytofirmans* PsJN is associated with an *iacR2*-encoded LysR-type regulator that would respond to a late metabolite (DOAA) of the IAA pathway, controlling transcription of *iac* genes related to later steps of IAA degradation and catechol *ortho*-ring cleavage (Fig. 3B) but also driving transcription of a putative two-component regulatory system, which apparently responds to the IAA molecule and regulates *iac* genes encoding early IAA degradation steps (Fig. 3B), thus suggesting complex regulatory mechanisms that would perfectly be operative in other *iac* gene-harboring bacteria (12) for controlling toxic intermediate accumulation and also IAA intermediate degradation.

Interestingly, it has been reported in *Arabidopsis thaliana* roots that 2-oxindole-3-acetic acid is a major primary IAA degradation metabolite (60), which is an isomer of the 2-hydroxyindole-3-acetic acid intermediate from the bacterial IAA degradation pathway (Fig. 1B), and DOAA derivatives which might regulate endogenous levels of IAA were detected in *Citrus sinensis* and *Vicia faba* (61, 62). Remarkably, *A. thaliana* plants exposed to IAA and to DOAA showed similar behavior (see Fig. S9 in the supplemental material), suggesting that this class of molecules is recognized by plants and could be present in plant root exudates and, therefore, available for plant-related bacteria carrying *iac* genes, including transporter- and tautomerase-related genes, participating in uptake and isomerization of DOAA-related molecules to be channeled through *iac* gene-encoded degradation.

The complex regulatory mechanisms in this PGPR could be related to its ecological importance and may be linked with its previously reported ability to synthesize IAA (19, 20, 22), raising questions about expression/coordination of IAA degradation and synthesis in natural environments.

MATERIALS AND METHODS

Bacterial strains, plasmids, and growth conditions. Bacteria and plasmids used in this study are listed in Table 1. *P. phytofirmans* and its derivatives were grown at 30°C in mineral salts medium (63), supplemented with 2.5, 5, or 10 mM benzoate (Bz), IAA, or fructose, plus the appropriate antibiotics, kanamycin (Km; 50 μg ml^{-1}), gentamicin (Gm; 30 μg ml^{-1}), or spectinomycin (Sp; 100 μg ml^{-1}). *Cupriavidus pinatubonensis* JMP134 (Table 1) and its derivatives were grown under the same conditions. *Escherichia coli* Mach (Invitrogen, Carlsbad, CA, USA) was grown at 37°C in Luria-Bertani (LB) medium. Growth was measured by optical density at 600 nm (OD_{600}). For preparation of a nitrogen-free mineral salts medium, $(NH_4)_2SO_4$ was removed and $Ca(NO_3)_2{\cdot}4H_2O$ was replaced by $CaSO_4{\cdot}2H_2O$ (63). At least three biological replicates were performed for each growth measurement. Growth yield averages were estimated considering an OD_{600} of 0.6 equivalent to 0.1 mg of cells, based on the information that average bacterial weight is 10^{-12} g (64) and that an OD_{600} of 0.6 in strain PsJN corresponds to approximately 1×10^8 cells/ml.

Chromosomal disruption of gene sequences in *P. phytofirmans* PsJN. Internal fragments of *iac* and associated genes (*iacA*, *iacA2*, *iacB*, *iacC*, *iacD*, *iacE*, *iacF*, *iacG*, *iacG2*, *iacH*, *iacI*, *iacS*, *iacR1*, *iacR2*, *iacY*, *iacT1*, *iacT2*, and *catA*) were amplified by PCR, using primer pairs listed in Table 2. The PCR products were cloned using the pCR2.1-TOPO system (Invitrogen, Carlsbad, CA, USA) to generate plasmids listed in Table 1. For gene inactivation, suicidal pCR2.1*iac* or pCR2.1*catA* plasmids (Table 1) were electroporated in *P. phytofirmans* PsJN to get a one-recombination-event disruption of the target gene, resulting in mutants (Table 1) which were selected on LB agar containing 50 μg ml^{-1} Km. Correct insertions in all mutants were confirmed by PCR using primer pairs located in genomic DNA and suicidal plasmid DNA and subsequent sequencing.

Detection of transcripts by quantitative real-time PCR. Cells of *P. phytofirmans* were grown on 2.5 mM fructose, Bz, or IAA as the sole carbon and energy source. Then, total RNA was obtained from 4 ml of mid-log-phase cells, using RNAprotect bacterial reagent and the RNeasy minikit (Qiagen, Chatsworth, CA, USA). The RNA was quantified using an Eon microplate spectrophotometer (BioTek, Winooski, VT, USA) and treated with the Turbo DNase kit (Ambion, Austin, TX, USA) to remove DNA contamination. The reverse transcription-PCR was performed using the ImProm-II reverse transcription system (Promega Corporation, Madison, WI, USA) with 1 μg of RNA in 20-μl reaction mixtures. Real-time PCR was performed using the Power SYBR green PCR master mix (Applied Biosystems, Warrington, UK) and Eco real-time PCR detection system (Illumina, San Diego, CA, USA). The PCR mixture (15 μl) contained 3.0 μl of template cDNA (diluted 1:10) and 0.2 μM (each) primer. Amplification was performed under the following conditions: 95°C for 10 min, followed by 40 cycles of 95°C for 30 s, 60°C for 30 s, and 72°C for 40 s, and finishing with a melting cycle from 55 to 95°C. Relative gene expression values were calculated using the comparative cycle threshold (C_T) method (also known as the $2^{-\Delta\Delta CT}$ method) (65). 16S rRNA gene sequence (Bphyt_R0071) was used as a reference gene (internal control) in these assays. Gene expression levels were normalized to the average value of the gene expression levels determined in the fructose treatment. Genes analyzed by quantitative real-time PCR were *iacA* (Bphyt_2161), *iacC* (Bphyt_2156), *iacF* (Bphyt_2150), *iacG* (Bphyt_2167), *iacA2* (Bphyt_6911), *catA* (Bphyt_2152), *catA2* (Bphyt_1590), *iacR1* (Bphyt_2166), *iacR2* (Bphyt_2155), *iacS* (Bphyt_2160), the 30S ribosomal protein S7 (rpS7) gene (Bphyt_3648), and *kynA* (Bphyt_3229). The latter two gene sequences were also used as gene expression controls. Experiments were done in three biological replicates.

Construction of plasmid derivatives expressing *iac* genes. To obtain pBS1-*iacABIHECDGF* plasmid (pBS1-*iac*1), which contains the complete *iac* gene cluster under the control of an arabinose-inducible promoter, the Gibson et al. assembly method was used (66). In brief, PCR products comprising *iacABIHE* (primer pair 1-2), *iacCD* (primer pair 3-4), *iacG* (primer pair 5-6), and *iacF* (primer pair 7-8) genes and pBS1 plasmid (primer pair 9-10) (67) were obtained using primer pairs listed in Table 2. These primers contain a 20-bp terminal sequence homologous to the terminus of the fragment to be linked, and the sequences were combined and ligated to generate a new DNA molecule in a one-step isothermal reaction (66). Also, PCR products lacking one or two of these *iac* genes were amplified using primer pairs listed in Table 2: *iacBIHE* (primer pair 2-11), *iacCD* (primer pair 3-4), *iacG* (primer pair 5-6), and *iacF* (primer pair 7-8) genes were used to obtain the *iac*1ΔA derivative; *iacA* (primer pair 1-12), *iacIHE* (primer pair 2-13), *iacCD* (primer pair 3-4), *iacG* (primer pair 5-6), and *iacF* (primer pair 7-8) genes were used to produce the *iac*1ΔB derivative; *iacABIHE* (primer pair 1-15), *iacG* (primer pair 5-6), and *iacF* (primer pair 7-8) genes were used to produce the *iac*1ΔCD derivative; *iacABIH* (primer pair 1-14), *iacCD* (primer pair 3-4), *iacG* (primer pair 5-6), and *iacF* (primer pair 7-8) genes were used to give the *iac*1ΔE derivative; *iacABIHE* (primer pair 1-2), *iacCD* (primer pair 3-4), and *iacG* (primer pair 5-16) genes were used to create the *iac*1ΔF derivative; *iacABIHE* (primer pair 1-2), *iacCD* (primer pair 3-4), and *iacF* (primer pair 8-17) genes were used to generate the *iac*1ΔG derivative; *iacABI* (primer pair 1-18), *iacE* (primer pair 2-19), *iacCD* (primer pair 3-4), *iacG* (primer pair 5-6), and *iacF* (primer pair 7-8) genes were used to make the *iac*1ΔH derivative; and *iacAB* (primer pair 1-20), *iacHE* (primer pair 2-21), *iacCD* (primer pair 3-4), *iacG* (primer pair 5-6), and *iacF* (primer pair 7-8) genes were used to yield the *iac*1ΔI derivative. In addition, expression plasmids containing single or combinations of some *iac* genes (Table 1) were generated, using primer pairs listed in Table 2: for *iacA*, primer pair 1-22; *iacAG*, primer pairs 1-23 and 5-16; *iacA2*, primer pair 24-25; *iacA2G2*,

TABLE 1 Bacterial strains and plasmids used in this study

Strain or plasmid	Relevant phenotype and/or genotype[a]	Reference or source
Paraburkholderia phytofirmans strains		
PsJN	IAA$^+$ Bz$^+$ fructose$^+$	17
PsJN::pCR2.1*iacA*	IAA$^-$ Km^r	This study
PsJN::pCR2.1*iacB*	IAA$^-$ Km^r	This study
PsJN::pCR2.1*iacC*	IAA$^-$ Km^r	This study
PsJN::pCR2.1*iacD*	IAA$^-$ Km^r	This study
PsJN::pCR2.1*iacE*	IAA$^-$ Km^r	This study
PsJN::pCR2.1*iacF*	IAA$^-$ Km^r	This study
PsJN::pCR2.1*iacG*	IAA$^+$ Km^r	This study
PsJN::pCR2.1*iacH*	IAA$^-$ Km^r	This study
PsJN::pCR2.1*iacI*	IAA$^-$ Km^r	This study
PsJN::pCR2.1*iacA2*	IAA$^+$ Km^r	This study
PsJN::pCR2.1*iacG2*	IAA$^+$ Km^r	This study
PsJN::pCR2.1*iacT1*	IAA$^+$ Km^r	This study
PsJN::pCR2.1*iacT2*	IAA$^+$ Km^r	This study
PsJN::pCR2.1*iacY*	IAA$^+$ Km^r	This study
PsJN::pCR2.1*iacS*	IAA$^+$ Km^r	This study
PsJN::pCR2.1*iacR1*	IAA$^-$ Km^r	This study
PsJN::pCR2.1*iacR2*	IAA$^-$ Km^r	This study
PsJN::pCR2.1*catA*	IAA$^-$ Bz$^+$ Km^r	This study
Other strains		
Cupriavidus pinatubonensis		
JMP134	IAA$^-$ fructose$^+$	DSMZ (28)
JMP134*iac*1	Strain expressing *iacABIHECDGF* genes driven by the heterologous P_{BAD} promoter, Gm$^+$	This study
Escherichia coli Mach	Δ*recA1398 endA1 tonA* ϕ80Δ*lacM15* Δ*lacX74 hsdR*(r_K^- m_K^+)	Invitrogen, Carlsbad, CA, USA
Plasmids		
pCR2.1-TOPO	Suicide vector in *P. phytofirmans* PsJN, Ap^r Km^r	Invitrogen, Carlsbad, CA, USA
pCR2.1*iac*[b]	pCR2.1 derivatives with internal fragment of *iac* genes, Ap^r Km^r	This study
pCR2.1*catA*	pCR2.1 derivative with internal fragment of *catA* gene, Ap^r Km^r	This study
pKGWP0	BHR *lacZ* transcriptional fusion vector, Sp^r	68
placA-*lacZ*	P_{iacA} pKGWP0 derivative Sp^r	This study
placC-*lacZ*	P_{iacC} pKGWP0 derivative Sp^r	This study
placF-*lacZ*	P_{iacF} pKGWP0 derivative Sp^r	This study
placG-*lacZ*	P_{iacG} pKGWP0 derivative Sp^r	This study
pCatB-*lacZ*	P_{catB} pKGWP0 derivative Sp^r	This study
pBS1	BHR gateway destination vector, *araC*-P_{BAD} Gm^r	67
pBS1*iac*1	*iacABIHECDGF*-expressing pBS1 derivative, Gm^r	This study
pBS1*iac*1ΔA	*iacBIHECDGF*-expressing pBS1 derivative, Gm^r	This study
pBS1*iac*1ΔB	*iacAIHECDGF*-expressing pBS1 derivative, Gm^r	This study
pBS1*iac*1ΔCD	*iacABIHEGF*-expressing pBS1 derivative, Gm^r	This study
pBS1*iac*1ΔE	*iacABIHCDGF*-expressing pBS1 derivative, Gm^r	This study
pBS1*iac*1ΔF	*iacABIHECDG*-expressing pBS1 derivative, Gm^r	This study
pBS1*iac*1ΔG	*iacABIHECDF*-expressing pBS1 derivative, Gm^r	This study
pBS1*iac*1ΔH	*iacABIECDGF*-expressing pBS1 derivative, Gm^r	This study
pBS1*iac*1ΔI	*iacABHECDGF*-expressing pBS1 derivative, Gm^r	This study
pBS1-iacA	*iacA*-expressing pBS1 derivative, Gm^r	This study
pBS1-iacAG	*iacAG*-expressing pBS1 derivative, Gm^r	This study
pBS1-iacA2	*iacA2*-expressing pBS1 derivative, Gm^r	This study
pBS1-iacA2G2	*iacA2G2*-expressing pBS1 derivative, Gm^r	This study
pBS1-iacE	*iacE*-expressing pBS1 derivative, Gm^r	This study
pBS1-iacB	*iacB*-expressing pBS1 derivative, Gm^r	This study
pBS1-iacEB	*iacEB*-expressing pBS1 derivative, Gm^r	This study
pBS1-iacC	*iacC*-expressing pBS1 derivative, Gm^r	This study
pBS1-iacCD	*iacCD*-expressing pBS1 derivative, Gm^r	This study
pBS1-iacCDF	*iacCDF*-expressing pBS1 derivative, Gm^r	This study
pBS1-iacCDFI	*iacCDFI*-expressing pBS1 derivative, Gm^r	This study
pBS1-iacH	*iacH*-expressing pBS1 derivative, Gm^r	This study
p0-iacYT1	*iacYT1*-expressing pKGWP0 derivative, Sp^r	This study

[a]IAA$^+$, Bz$^+$, and fructose$^+$, ability to grow on indole-3-acetate, benzoate, and fructose, respectively; Ap^r, Gm^r, Km^r, and Sp^r, resistance to ampicillin, gentamicin, kanamycin, and spectinomycin, respectively; BHR, broad host range.

[b]Internal fragments of *iacA*, *iacB*, *iacC*, *iacD*, *iacE*, *iacF*, *iacG*, *iacH*, *iacI*, *iacA2*, *iacG2*, *iacT1*, *iacT2*, *iacY*, *iacS*, *iacR1*, and *iacR2* cloned in pCR2.1 plasmid, to obtain their respective derivatives.

TABLE 2 Primer pairs used in this study

	Forward		Reverse	
Purpose	Primer name	Sequence (5′→3′)	Primer name	Sequence (5′→3′)
Inactivation of genes	Mut iacAFw	GCCCAGTTTCTCGACATGAT	Mut iacARv	GTCGTCTGCAACGAACTGGT
	Mut iacBFw	CGAACAGATCGGCGAAGT	Mut iacBRv	CATAGCGCCACAGGTTGTATT
	Mut iacCFw	GGTCA ACGTCTTGCA GAACC	Mut iacCRv	GTTTCGTCGTCGATCGATTT
	Mut iacDFw	GACTATCGCGAGTGGCTCA	Mut iacDRv	CTTGCAAAACTGATGCGATG
	Mut iacEFw	AAGTCGTCTCCGTGATGGAC	Mut iacERv	GATCACCGCCTTCAGTTTGT
	Mut iacFFw	AACAGGAGCGCTTCGTATTG	Mut iacFRv	GCAAACCGTTCGAGATGAAT
	Mut iacGFw	TCGACGTCAAACAGCAATTC	Mut iacGRv	ACCGAAGCGTTCTTCCATC
	Mut iacHFw	ATCGGATTGAAGCCCACTTT	Mut iacHRv	CGAGGTCTCGACATTGATGA
	Mut iacIFw	GAAATTCTCGCGATGCTCAC	Mut iacIRv	GAAAGTGCGTGATGAACCAG
	Mut iacA2Fw	GTCGAGAACTGGAACGTGGT	Mut iacA2Rv	CAGTTGGCTTCTGCTTTCG
	Mut iacG2Fw	CCAGCTACGTGCATGACATC	Mut iacG2Rv	AATCTGCGCAAACATGACC
	Mut iacT1Fw	GGTGGAAAGCTTCATGTCGT	Mut iacT1Rv	GAGGAACACCAGCATTGGTT
	Mut iacT2Fw	AGCATTCTGCTGATTCACGA	Mut iacT2Rv	TTGAGAACGCGAAGAAGATG
	Mut iacYFw	ATTGATCGCGGCTCTCAC	Mut iacYRv	GCGATCAAGGCTTCTTTTTG
	Mut iacSFw	TCAGCGTGGAAGACACACTC	Mut iacSRv	GTTGTAACGTCCGGCGTATT
	Mut iacR1Fw	GTGCAAGCGGAGTTGAATC	Mut iacR1Rv	CTTCACGCTGATCGACAGAT
	Mut iacR2Fw	CGCTGGAACTGTCGACTATC	Mut iacR2Rv	GAAACGCCTTCAAACTCAGC
	Mut catAFw	TCTGGGTTTCGAGCATTTTC	Mut catARv	CGGAAGCTGTATTTGCCTTC
RT-PCR[a] analysis	iacA intFw	GCCCAGTTTCTCGACATGAT	iacA intRv	AGATTTCCGCTTGTGTATGC
	iacC intFw	GATGGTTATGAAGGCGTGGT	iacC intRv	GGCTCGATCTCCTGATTGAA
	iacF intFw	CTGATGCGATTCATCTCGAA	iacF intRv	ATGGTCGTGTCCTTGTCCAC
	iacG intFw	GCGACTTTCCAGAGCAACC	iacG intRv	ACCGAAGCGTTCTTCCATC
	iacA2 intFw	GTCGAGAACTGGAACGTGGT	iacA2 intRv	CAGTTGGCTTCTGCTTTCG
	iacR1intFw	GTGCAAGCGGAGTTGAATC	iacR1intRv	CTTCACGCTGATCGACAGAT
	iacR2intFw	CGCTGGAACTGTCGACTATC	iacR2intRv	GAAACGCCTTCAAACTCAGC
	iacSintFw	TTGTCCCTTCGTTTGTCCTT	iacSintRv	CCAGGTGGTGTTGAATCTGG
	catA intFw	ACGTACAACGGACCTTCGAT	catA intRv	TCTGGGTTTCGAGCATTTTC
	catA2 intFw	TTCAACAAGCTCGGACAGG	catA2 intRv	ACATACAGCGGACCTTCGAT
	kynA intFw	TGAAGCTCGCGTTGTATGAG	kynA intRv	TCCGATAAACCTCCAACCAG
	rpS7 intFw	CGAACAGATCCAGACCAAGG	rpS7 intRv	ACTTCTCGCTGCGCTTCTT
	16S intFw	CGGGCTAGAGTATGGCAGAG	16S intRv	CGTGCATGAGCGTCAGTATT

(Continued on next page)

TABLE 2 (Continued)

	Forward		Reverse	
Purpose	Primer name	Sequence (5′→3′)	Primer name	Sequence (5′→3′)
Transcriptional fusions	PiacA Fw	GCGCGGTACCCAGGCGGTGAAAGTCTTCTT	PiacA Rv	TGTCCTCGAGGGTGAGGTATCTCCTTGATTCG
	PiacC Fw	GCGCGGTACCGAATGAAAAGCGGGTCGTC	PiacC Rv	TCGCCTCGAGCTTGTGTAGGTGGGGGTGGT
	PiacF Fw	TAGAGGTACCGATTTGAATGTTCCGACTGGA	PiacF Rv	CGTTCTCGAGGGTTCTTTCTATGAGCTTGC
	PiacG Fw	TTATGGTACCCGAAGGCTGGGACATGGT	PiacG Rv	ATTTCTCGAGGATTCCTCGGGCAGGTGT
	PcatB Fw	GTTTGGTACCTTCCTCGATCTGCT GGATCT	PcatB Rv	ATTCCTCGAGCTCCTGAACTGCCTGACCTG
iac gene expression	1 (iacABIHE Fw)	TTGGGCTAGCGAATTCCTGCTTACGTTTCGATCCAACTTGC	2 (iacABIHE Rv)	GTGGTCGATGAAGCGAAGTCGTCAGCGCATGAAGAGTCC
	3 (iacCD Fw)	GACTTCGCTTCATCGACCAC	4 (iacCD Rv)	CAGGTGTCGAGTGGTTTGATTTCGAAAAGATCAAAGCAGGAA
	5 (iacG Fw)	AATCAAACCACTCGACACCTG	6 (iacG Rv)	GGTTGTGCGTCAAGGATAAGCCACTGTGCGTAATCAATGC
	7 (iacF Fw)	CTTATCCTTGACGCACAACC	8 (iacF Rv)	GTAATACGACTCACTATAGGAAGAAAAGGCGCTTGTGAAA
	9 (pBS1 Fw)	CCTATAGTGAGTCGTATTAC	10 (pBS1 Rv)	GCAGGAATTCGCTAGCCCAA
	11 (iacB Fw)	TTGGGCTAGCGAATTCCTGCCTATCCGCACAACCAGGATT	12 (iacA Rv)	AATCCTGGTTGTGCGGATAG
	13 (iacI Fw)	CTATCCGCACAACCAGGATTCTTGAGCGTTTCGGAACAAC	14 (iacH Rv)	GTGGTCGATGAAGCGAAGTCCCACTCCACTTCGAAATAACG
	15 (iacE Rv)	CAGGTGTCGAGTGGTTTGATTATGCCGCTTTGGTGTTGT	16 (iacG Rv2)	GTAATACGACTCACTATAGGCCACTGTGCGTAATCAATGC
	17 (iacF Fw2)	TTCCTGCTTTGATCTTTTCGACTTATCCTTGACGCACAACC	18 (iacI Rv)	CCTATCGACAGCGTCTGGA
	19 (iacE Fw)	TCCAGACGCTGTCGATAGGGCCGTTATTTCGAAGTGGAG	20 (iacB Rv)	TCCTGGTTCGCGTTCATT
	21 (iacH Fw)	AATGAACGCGAACCAGGAAGGTCAACGCAAGGAAACC	22 (iacA Rv2)	GTAATACGACTCACTATAGGAATCCTGGTTGTGCGGATA
	23 (iacA Rv3)	CAGGTGTCGAGTGGTTTGATTAATCCTGGTTGTGCGGATAG	24 (iacA2 Fw)	TTGGGCTAGCGAATTCCTGCAGCTTCTCCTGTACCGATCC
	25 (iacA2 Rv)	GTAATACGACTCACTATAGGTTCCTTTTCCTTTTGCATGG	26 (iacG2 Rv)	GTAATACGACTCACTATAGGGATGAAAGATCCGGAGAGCA
	27 (iacE Fw2)	TTGGGCTAGCGAATTCCTGCGCCGTTATTTCGAAGTGGAG	28 (iacE Rv2)	GTAATACGACTCACTATAGGATGCCGCTTTGGTGTTGT
	29 (iacB Rv2)	GTAATACGACTCACTATAGGTCCTGGTTCGCGTTCATT	30 (iacE Fw3)	AATGAACGCGAACCAGGAGCCGTTATTTCGAAGTGGAG
	31 (iacC Fw)	TTGGGCTAGCGAATTCCTGCGACTTCGCTTCATCGACCAC	32 (iacC Rv)	GTAATACGACTCACTATAGGAGCGTGTTTCTGTCGTCCAT
	33 (iacD Rv)	GTAATACGACTCACTATAGGTCGAAAAGATCAAAGCAGGAA	34 (iacF Rv1)	AAGAAAAGGCGCTTGTGAA
	35 (iacI Fw2)	TTTCACAAGCGCCTTTTCTTCTTGAGCGTTTCGGAACAAC	36 (iacI Rv2)	GTAATACGACTCACTATAGGCCTATCGACAGCGTCTGGA
	37 (iacH Fw2)	TTGGGCTAGCGAATTCCTGCAGGTCAACGCAAGGAAACC	38 (iacH Rv2)	GTAATACGACTCACTATAGGCCACTCCACTTCGAAATAACG
	39 (iacY Fw)	ACAGGATGAGGATCGTTTCGATCGGCTTCCTGCTTTGAT	40 (iacT1 Rv)	CAAGAAAGCTGGGTCGAATTGGCTCGAATGCAGCTTCTC
	41 (pKan Fw)	CTAAGTAAGTAAGGAGAAGGGCGGGCTATCTGGACAAGGGAAA	42 (pKan Rv)	CGAAACGATCCTCATCCTGT
	43 (p0 Fw1)	AATTCGACCCAGCTTTCTTG	44 (p0 Rv1)	CCTTTGAGTGAGCTGATACCG
	45 (p0 Fw2)	CGGTATCAGCTCACTCAAAGG	46 (p0 Rv2)	CGCCCTTCTCCTTACTTACTTAG

[a]RT-PCR, reverse transcription-PCR.

primer pair 24-26; *iacE*, primer pair 27-28; *iacB*, primer pair 11-29; *iacEB*, primer pairs 11-20 and 28-30; *iacC*, primer pair 31-32; *iacCD*, primer pair 31-33; *iacCDF*, primer pairs 4-31 and 8-17; *iacCDFI*, primer pairs 4-31, 17-34, and 35-36; *iacH*, primer pair 37-38; and *iacYT1*, primer pair 39-40. With the exception of *iacYT1* genes, all fragments containing the 20-bp terminal sequence that overlapped each other were ligated to pBS1 plasmid (primer pair 9-10), using the Gibson et al. assembly method (66), to get plasmids that contain *iac* genes under the control of the AraBAD (P_{BAD}) promoter in pBS1 (67). Additionally, the *iacYT1* genes were ligated to pKGWP0 plasmid (68) lacking the *lacZ* gene (primer pairs 43-44 and 45-46), to which the constitutive promoter of kanamycin phosphotransferase of plasmid pCR2.1-TOPO (primer pair 41-42) was added to obtain constitutive expression of the *iacYT1* genes, using the Gibson et al. assembly method (66). Plasmid pBS1 or pKGWP0 derivatives were electroporated in *C. pinatubonensis* JMP134 and selected in LB medium plus Gm (30 μg/ml) or Sp (100 μg/ml), respectively. For expression of *iac* genes driven by the heterologous P_{BAD} promoter, these derivatives were exposed to 5 mM L-arabinose, which is not a carbon source for *C. pinatubonensis* JMP134. All plasmid constructions obtained by the Gibson et al. assembly method were confirmed by sequencing.

Construction of *lacZ* reporter fusions. Putative promoter regions were fused to the *lacZ* gene of pKGWP0 (68). PCR products comprising approximately 200 bp of the upstream region contiguous to translational starts of the *iacA*, *iacC*, *iacF*, *iacG*, or *catB* genes were obtained, using primer pairs listed in Table 2. The amplified DNA fragments were cloned into the XhoI-KpnI restriction site of pKGWP0, forming placA-lacZ, placC-lacZ, placF-lacZ, placG-lacZ, and pCatB-lacZ plasmids; transferred into *P. phytofirmans* and its derivatives; and selected in minimal medium supplemented with 100 μg ml^{-1} Sp. To evaluate promoter induction profiles, bacteria carrying promoter constructions were grown overnight on 10 mM fructose, refreshed in the same medium to an OD_{600} of 0.2, and then induced during 6 h with 0.25 mM IAA and/or compounds X and Y or DOAA. Compounds X and Y and DOAA were prepared using 4-fold-diluted supernatants of strain JMP134-*iacAG* or JMP134*iac*1 resting cells previously exposed for 2 h to 1 mM IAA as the only carbon source, respectively. β-Galactosidase assays were performed according to standard protocols (69).

Analytical methods. The presence of IAA and its intermediates was determined by high-performance liquid chromatography–UV detection (HPLC-UV) using cell-free supernatants from cells exposed to IAA. Samples (20 μl) were injected into a Hitachi LaChrom Elite high-performance liquid chromatograph (Tokyo, Japan) equipped with a Kromasil 100-3.5 C_{18} 4.6-μm-diameter column. Methanol-H_2O mixtures containing 0.1% (vol/vol) phosphoric acid were used as the solvent, at a flow rate of 1 ml min^{-1}. The column effluent was monitored at 210 nm. Retention times with methanol-H_2O (40:60) for IAA, catechol, and compound 1 (DOAA) were 6.75, 3.05, and 2.04 min, respectively, whereas retention times with methanol-H_2O (80:20) for IAA and compound 1 were 3.18 and 1.03 min, respectively.

In order to identify compound 1 (DOAA), this intermediate was produced and accumulated in strain JMP134*iac*1 exposed to 2.5 mM IAA as the sole carbon source for 2 h. Then, cells were centrifuged at 9,000 rpm, supernatant containing compound 1 was filtered (filter unit of 0.22 μm), and its pH was lowered to 2.5 using hydrochloric acid. Then, compound 1 was extracted from the aqueous medium with 1 volume of ethyl acetate (three times). The pooled organic layer was dried over anhydrous Na_2SO_4 and filtered, and the solvent vacuum were removed. The crude product was subjected to spectroscopic analysis. NMR spectra were recorded on a Bruker Advance III HD 400 instrument at 400 MHz for ^{1}H and 100 MHz for ^{13}C, using the solvent signal of dimethyl sulfoxide (DMSO)-D_6 as reference. The chemical shifts are expressed in parts per million (ppm) (δ scale) downfield from tetramethylsilane, and coupling constant values (J) are given in hertz. The IR spectrum was obtained on a Bruker Vector 22 spectrophotometer, using KBr discs. The mass spectra were determined in a TQ 4500 triple-quadrupole mass spectrometer coupled with electrospray ionization operated in the negative ion mode.

Bioinformatic tools. The *iac* gene sequences were retrieved from the Integrated Microbial Genomes database (https://img.jgi.doe.gov/cgi-bin/m/main.cgi). Protein similarity and conserved domain searches were performed with the BLASTP program and the Conserved Domains Database from the NCBI website using default parameters (70, 71). Only proteins of *P. phytofirmans* PsJN displaying at least 30% amino acid identity with *iac* genes of *P. putida* 1290 were considered for analysis.

Chemicals. IAA, indole, and catechol were obtained from Sigma-Aldrich (Steinheim, Germany). Bz, fructose, and L-arabinose were purchased from Merck (Darmstadt, Germany).

SUPPLEMENTAL MATERIAL

Supplemental material for this article may be found at https://doi.org/10.1128/AEM.01991-16.

TEXT S1, PDF file, 1.3 MB.

ACKNOWLEDGMENTS

The work was funded by FONDECYT grants 1110850 and 1151130, CONICYT grant FB 0002-2014, Millennium Nuclei in Plant Functional Genomics grant P10-062F, and Plant Systems and Synthetic Biology grant NC130030.

REFERENCES

1. Schaller GE, Bishopp A, Kieber JJ. 2015. The yin-yang of hormones: cytokinin and auxin interactions in plant development. Plant Cell 27:44–63. https://doi.org/10.1105/tpc.114.133595.
2. Vanneste S, Friml J. 2009. Auxin: a trigger for change in plant development. Cell 136:1005–1016. https://doi.org/10.1016/j.cell.2009.03.001.
3. Tromas A, Perrot-Rechenmann C. 2010. Recent progress in auxin biology. Crit Rev Biol 333:297–306. https://doi.org/10.1016/j.crvi.2010.01.005.
4. Duca D, Lorv J, Patten CL, Rose D, Glick BR. 2014. Indole-3-acetic acid in plant-microbe interactions. Antonie Van Leeuwenhoek 106:85–125. https://doi.org/10.1007/s10482-013-0095-y.
5. Patten CL, Blakney AJ, Coulson TJ. 2013. Activity, distribution and function of indole-3-acetic acid biosynthetic pathways in bacteria. Crit Rev Microbiol 39:395–415. https://doi.org/10.3109/1040841X.2012.716819.
6. Spaepen S, Vanderleyden J. 2011. Auxin and plant-microbe interactions. Cold Spring Harb Perspect Biol 3:a001438. https://doi.org/10.1101/cshperspect.a001438.
7. Arora PK, Sharma A, Bae H. 2015. Microbial degradation of indole and its derivatives. J Chem 2015:129159. https://doi.org/10.1155/2015/129159.
8. Ebenau-Jehle C, Thomas M, Scharf G, Kockelkorn D, Knapp B, Schühle K, Heider J, Fuchs G. 2012. Anaerobic metabolism of indoleacetate. J Bacteriol 194:2894–2903. https://doi.org/10.1128/JB.00250-12.
9. Egebo LA, Nielsen SV, Jochimsen BU. 1991. Oxygen-dependent catabolism of indole-3-acetic acid in *Bradyrhizobium japonicum*. J Bacteriol 173:4897–4901.
10. Jensen JB, Egsgaard H, Van Onckelen H, Jochimsen BU. 1995. Catabolism of indole-3-acetic acid and 4- and 5-chloroindole-3-acetic acid in *Bradyrhizobium japonicum*. J Bacteriol 177:5762–5766.
11. Leveau JH, Lindow SE. 2005. Utilization of the plant hormone indole-3-acetic acid for growth by *Pseudomonas putida* strain 1290. Appl Environ Microbiol 71:2365–2371. https://doi.org/10.1128/AEM.71.5.2365-2371.2005.
12. Leveau JH, Gerards S. 2008. Discovery of a bacterial gene cluster for catabolism of the plant hormone indole 3-acetic acid. FEMS Microbiol Ecol 65:238–250. https://doi.org/10.1111/j.1574-6941.2008.00436.x.
13. Lin GH, Chen HP, Huang JH, Liu TT, Lin TK, Wang SJ, Tseng CH, Shu HY. 2012. Identification and characterization of an indigo-producing oxygenase involved in indole 3-acetic acid utilization by *Acinetobacter baumannii*. Antonie Van Leeuwenhoek 101:881–890. https://doi.org/10.1007/s10482-012-9704-4.
14. Scott JC, Greenhut IV, Leveau JH. 2013. Functional characterization of the bacterial *iac* genes for degradation of the plant hormone indole-3-acetic acid. J Chem Ecol 39:942–951. https://doi.org/10.1007/s10886-013-0324-x.
15. Shu HY, Lin LC, Lin TK, Chen HP, Yang HH, Peng KC, Lin GH. 2015. Transcriptional regulation of the *iac* locus from *Acinetobacter baumannii* by the phytohormone indole-3-acetic acid. Antonie Van Leeuwenhoek 107:1237–1247. https://doi.org/10.1007/s10482-015-0417-3.
16. Sawana A, Adeolu M, Gupta RS. 2014. Molecular signatures and phylogenomic analysis of the genus *Burkholderia*: proposal for division of this genus into the emended genus *Burkholderia* containing pathogenic organisms and a new genus *Paraburkholderia* gen. nov. harboring environmental species. Front Genet 5:429. https://doi.org/10.3389/fgene.2014.00429.
17. Mitter B, Petric A, Shin MW, Chain PS, Hauberg-Lotte L, Reinhold-Hurek B, Nowak J, Sessitsch A. 2013. Comparative genome analysis of *Burkholderia phytofirmans* PsJN reveals a wide spectrum of endophytic lifestyles based on interaction strategies with host plants. Front Plant Sci 4:120. https://doi.org/10.3389/fpls.2013.00120.
18. Poupin MJ, Timmermann T, Vega A, Zúñiga A, González B. 2013. Effects of the plant growth-promoting bacterium *Burkholderia phytofirmans* PsJN throughout the life cycle of *Arabidopsis thaliana*. PLoS One 8:e69435. https://doi.org/10.1371/journal.pone.0069435.
19. Sun Y, Cheng Z, Glick BR. 2009. The presence of a 1-aminocyclopropane-1-carboxylate (ACC) deaminase deletion mutation alters the physiology of the endophytic plant growth-promoting bacterium *Burkholderia phytofirmans* PsJN. FEMS Microbiol Lett 296:131–136. https://doi.org/10.1111/j.1574-6968.2009.01625.x.
20. Zúñiga A, Poupin MJ, Donoso R, Ledger T, Guiliani N, Gutiérrez RA, González B. 2013. Quorum sensing and indole-3-acetic acid degradation play a role in colonization and plant growth promotion of *Arabidopsis thaliana* by *Burkholderia phytofirmans* PsJN. Mol Plant Microbe Interact 26:546–553. https://doi.org/10.1094/MPMI-10-12-0241-R.
21. Weilharter A, Mitter B, Shin MV, Chain PS, Nowak J, Sessitsch A. 2011. Complete genome sequence of the plant growth-promoting endophyte *Burkholderia phytofirmans* strain PsJN. J Bacteriol 193:3383–3384. https://doi.org/10.1128/JB.05055-11.
22. Naveed M, Qureshi MA, Zahir ZA, Hussain MB, Sessitsch A, Mitter B. 2015. L-Tryptophan-dependent biosynthesis of indole-3-acetic acid (IAA) improves plant growth and colonization of maize by *Burkholderia phytofirmans* PsJN. Ann Microbiol 65:1381–1389. https://doi.org/10.1007/s13213-014-0976-y.
23. Baty F, Flandrois JP, Delignette-Muller ML. 2002. Modeling the lag time of *Listeria monocytogenes* from viable count enumeration and optical density data. Appl Environ Microbiol 68:5816–5825. https://doi.org/10.1128/AEM.68.12.5816-5825.2002.
24. Schweigert N, Zehnder AJ, Eggen RI. 2001. Chemical properties of catechols and their molecular modes of toxic action in cells, from microorganisms to mammals. Environ Microbiol 3:81–91. https://doi.org/10.1046/j.1462-2920.2001.00176.x.
25. Ledger T, Pieper DH, González B. 2006. Chlorophenol hydroxylases encoded by plasmid pJP4 differentially contribute to chlorophenoxyacetic acid degradation. Appl Environ Microbiol 72:2783–2792. https://doi.org/10.1128/AEM.72.4.2783-2792.2006.
26. Pérez-Pantoja D, Ledger T, Pieper DH, González B. 2003. Efficient turnover of chlorocatechols is essential for growth of *Ralstonia eutropha* JMP134(pJP4) in 3-chlorobenzoic acid. J Bacteriol 185:1534–1542. https://doi.org/10.1128/JB.185.5.1534-1542.2003.
27. Harwood CS, Parales RE. 1996. The *beta*-ketoadipate pathway and the biology of self-identity. Annu Rev Microbiol 50:553–590. https://doi.org/10.1146/annurev.micro.50.1.553.
28. Lykidis A, Pérez-Pantoja D, Ledger T, Mavromatis K, Anderson IJ, Ivanova NN, Hooper SD, Lapidus A, Lucas S, González B, Kyrpides NC. 2010. The complete multipartite genome sequence of *Cupriavidus necator* JMP134, a versatile pollutant degrader. PLoS One 5:e9729. https://doi.org/10.1371/journal.pone.0009729.
29. Pérez-Pantoja D, De la Iglesia R, Pieper DH, González B. 2008. Metabolic reconstruction of aromatic compounds degradation from the genome of the amazing pollutant-degrading bacterium *Cupriavidus necator* JMP134. FEMS Microbiol Rev 32:736–794. https://doi.org/10.1111/j.1574-6976.2008.00122.x.
30. Pérez-Pantoja D, Donoso R, Agulló L, Córdova M, Seeger M, Pieper DH, González B. 2012. Genomic analysis of the potential for aromatic compounds biodegradation in *Burkholderiales*. Environ Microbiol 14:1091–1117. https://doi.org/10.1111/j.1462-2920.2011.02613.x.
31. Reddy VS, Shlykov MA, Castillo R, Sun EI, Saier MH, Jr. 2012. The major facilitator superfamily (MFS) revisited. FEBS J 279:2022–2035. https://doi.org/10.1111/j.1742-4658.2012.08588.x.
32. Whipp MJ, Camakaris H, Pittard AJ. 1998. Cloning and analysis of the *shiA* gene, which encodes the shikimate transport system of *Escherichia coli* K-12. Gene 209:185–192. https://doi.org/10.1016/S0378-1119(98)00043-2.
33. Huddleston JP, Burks EA, Whitman CP. 2014. Identification and characterization of new family members in the tautomerase superfamily: analysis and implications. Arch Biochem Biophys 564:189–196. https://doi.org/10.1016/j.abb.2014.08.019.
34. Whitman CP, Aird BA, Gillespie WR, Stolowich NJ. 1991. Chemical and enzymatic ketonization of 2-hydroxymuconate, a conjugated enol. J Am Chem Soc 113:3154–3162. https://doi.org/10.1021/ja00008a052.
35. Ghisla S, Thorpe C. 2004. Acyl-CoA dehydrogenases. A mechanistic overview. Eur J Biochem 271:494–508.
36. Galán B, Díaz E, Prieto MA, García JL. 2000. Functional analysis of the small component of the 4-hydroxyphenylacetate 3-monooxygenase of *Escherichia coli* W: a prototype of a new flavin:NAD(P)H reductase subfamily. J Bacteriol 182:627–636. https://doi.org/10.1128/JB.182.3.627-636.2000.
37. Kavanagh KL, Jörnvall H, Persson B, Oppermann U. 2008. Medium- and short-chain dehydrogenase/reductase gene and protein families: the SDR superfamily: functional and structural diversity within a family of metabolic and regulatory enzymes. Cell Mol Life Sci 65:3895–3906. https://doi.org/10.1007/s00018-008-8588-y.
38. Ferraro DJ, Gakhar L, Ramaswamy S. 2005. Rieske business: structure-

function of Rieske non-heme oxygenases. Biochem Biophys Res Commun 338:175–190. https://doi.org/10.1016/j.bbrc.2005.08.222.
39. Kweon O, Kim SJ, Baek S, Chae JC, Adjei MD, Baek DH, Kim YC, Cerniglia CE. 2008. A new classification system for bacterial Rieske non-heme iron aromatic ring-hydroxylating oxygenases. BMC Biochem 9:11. https://doi.org/10.1186/1471-2091-9-11.
40. Bullock TL, Clarkson WD, Kent HM, Stewart M. 1996. The 1.6 angstroms resolution crystal structure of nuclear transport factor 2 (NTF2). J Mol Biol 260:422–431. https://doi.org/10.1006/jmbi.1996.0411.
41. Lundqvist T, Rice J, Hodge CN, Basarab GS, Pierce J, Lindqvist Y. 1994. Crystal structure of scytalone dehydratase—a disease determinant of the rice pathogen, *Magnaporthe grisea*. Structure 2:937–944. https://doi.org/10.1016/S0969-2126(94)00095-6.
42. Hurtubise Y, Barriault D, Sylvestre M. 1998. Involvement of the terminal oxygenase beta subunit in the biphenyl dioxygenase reactivity pattern toward chlorobiphenyls. J Bacteriol 180:5828–5835.
43. Aliverti A, Pandini V, Pennati A, de Rosa M, Zanetti G. 2008. Structural and functional diversity of ferredoxin-NADP(+) reductases. Arch Biochem Biophys 474:283–291. https://doi.org/10.1016/j.abb.2008.02.014.
44. Kallio P, Sultana A, Niemi J, Mäntsälä P, Schneider G. 2006. Crystal structure of the polyketide cyclase AknH with bound substrate and product analogue: implications for catalytic mechanism and product stereoselectivity. J Mol Biol 357:210–220. https://doi.org/10.1016/j.jmb.2005.12.064.
45. Staswick PE, Serban B, Rowe M, Tiryaki I, Maldonado MT, Maldonado MC, Suza W. 2005. Characterization of an Arabidopsis enzyme family that conjugates amino acids to indole-3-acetic acid. Plant Cell 17:616–627. https://doi.org/10.1105/tpc.104.026690.
46. Coschigano PW, Young LY. 1997. Identification and sequence analysis of two regulatory genes involved in anaerobic toluene metabolism by strain T1. Appl Environ Microbiol 63:652–660.
47. Lau PC, Wang Y, Patel A, Labbé D, Bergeron H, Brousseau R, Konishi Y, Rawlings M. 1997. A bacterial basic region leucine zipper histidine kinase regulating toluene degradation. Proc Natl Acad Sci U S A 94:1453–1458. https://doi.org/10.1073/pnas.94.4.1453.
48. Achong GR, Rodriguez AM, Spormann AM. 2001. Benzylsuccinate synthase of *Azoarcus* sp. strain T: cloning, sequencing, transcriptional organization, and its role in anaerobic toluene and *m*-xylene mineralization. J Bacteriol 183:6763–6770. https://doi.org/10.1128/JB.183.23.6763-6770.2001.
49. Labbé D, Garnon J, Lau PC. 1997. Characterization of the genes encoding a receptor-like histidine kinase and a cognate response regulator from a biphenyl/polychlorobiphenyl-degrading bacterium, Rhodococcus sp. strain M5. J Bacteriol 179:2772–2776.
50. O'Leary ND, Mooney A, O'Mahony M, Dobson AD. 2014. Functional characterization of a StyS sensor kinase reveals distinct domains associated with intracellular and extracellular sensing of styrene in *Pseudomonas putida* CA-3. Bioengineering 5:114–122. https://doi.org/10.4161/bioe.28354.
51. Maddocks SE, Oyston PC. 2008. Structure and function of the LysR-type transcriptional regulator (LTTR) family proteins. Microbiology 154:3609–3623. https://doi.org/10.1099/mic.0.2008/022772-0.
52. Cao H, Krishnan G, Goumnerov B, Tsongalis J, Tompkins R, Rahme LG. 2001. A quorum sensing-associated virulence gene of *Pseudomonas aeruginosa* encodes a LysR-like transcription regulator with a unique self-regulatory mechanism. Proc Natl Acad Sci U S A 98:14613–14618. https://doi.org/10.1073/pnas.251465298.
53. Kim J, Kim JG, Kang Y, Jang JY, Jog GJ, Lim JY, Kim S, Suga H, Nagamatsu T, Hwang I. 2004. Quorum sensing and the LysR-type transcriptional activator ToxR regulate toxoflavin biosynthesis and transport in *Burkholderia glumae*. Mol Microbiol 54:921–934. https://doi.org/10.1111/j.1365-2958.2004.04338.x.
54. Lu Z, Takeuchi M, Sato T. 2007. The LysR-type transcriptional regulator YofA controls cell division through the regulation of expression of *ftsW* in *Bacillus subtilis*. J Bacteriol 189:5642–5651. https://doi.org/10.1128/JB.00467-07.
55. Craven SH, Ezezika OC, Haddad S, Hall RA, Momany C, Neidle EL. 2009. Inducer responses of BenM, a LysR-type transcriptional regulator from *Acinetobacter baylyi* ADP1. Mol Microbiol 72:881–894. https://doi.org/10.1111/j.1365-2958.2009.06686.x.
56. Ezezika OC, Collier-Hyams LS, Dale HA, Burk AC, Neidle EL. 2006. CatM regulation of the *benABCDE* operon: functional divergence of two LysR-type paralogs in *Acinetobacter baylyi* ADP1. Appl Environ Microbiol 72:1749–1758. https://doi.org/10.1128/AEM.72.3.1749-1758.2006.
57. Nishijyo T, Haas D, Itoh Y. 2001. The CbrA-CbrB two component regulatory system controls the utilization of multiple carbon and nitrogen sources in *Pseudomonas aeruginosa*. Mol Microbiol 40:917–931. https://doi.org/10.1046/j.1365-2958.2001.02435.x.
58. Hąc-Wydro K, Flasiński M. 2015. The studies on the toxicity mechanism of environmentally hazardous natural (IAA) and synthetic (NAA) auxin. The experiments on model *Arabidopsis thaliana* and rat liver plasma membranes. Colloids Surf B Biointerfaces 130:53–60. https://doi.org/10.1016/j.colsurfb.2015.03.064.
59. Pieper DH, Engesser KH, Knackmuss HJ. 1989. Regulation of catabolic pathways of phenoxyacetic acids and phenols in *Alcaligenes eutrophus* JMP134. Arch Microbiol 151:365–371. https://doi.org/10.1007/BF00406566.
60. Pencík A, Simonovik B, Petersson SV, Henyková E, Simon S, Greenham K, Zhang Y, Kowalczyk M, Estelle M, Zazímalová E, Novák O, Sandberg G, Ljung K. 2013. Regulation of auxin homeostasis and gradients in Arabidopsis roots through the formation of the indole-3-acetic acid catabolite 2-oxindole-3-acetic acid. Plant Cell 25:3858–3570. https://doi.org/10.1105/tpc.113.114421.
61. Chamarro J, Ostin A, Sandberg G. 2001. Metabolism of indole-3-acetic acid by orange (*Citrus sinensis*) flavedo tissue during fruit development. Phytochemistry 57:179–187. https://doi.org/10.1016/S0031-9422(01)00023-1.
62. Tsurumi S, Wada S. 1985. Identification of 3-(O-beta-glucosyl)-2-indolone-3-acetylaspartic acid as a new indole-3-acetic acid metabolite in *Vicia* seedlings. Plant Physiol 79:667–671. https://doi.org/10.1104/pp.79.3.667.
63. Dorn E, Hellwig M, Reineke W, Knackmuss HJ. 1974. Isolation and characterization of a 3-chlorobenzoate degrading pseudomonad. Arch Microbiol 99:61–70. https://doi.org/10.1007/BF00696222.
64. Scott TA, Mercer EI. 1996. Concise encyclopedia of biochemistry and molecular biology. Walter de Gruyter, Berlin, Germany.
65. Schmittgen TD, Livak KJ. 2008. Analyzing real-time PCR data by the comparative C_T method. Nat Protoc 3:1101–1108. https://doi.org/10.1038/nprot.2008.73.
66. Gibson DG, Young L, Chuang RY, Venter JC, Hutchison CA, III, Smith HO. 2009. Enzymatic assembly of DNA molecules up to several hundred kilobases. Nat Methods 6:343–345. https://doi.org/10.1038/nmeth.1318.
67. Bronstein PA, Marrichi M, Cartinhour S, Schneider DJ, DeLisa MP. 2005. Identification of a twin-arginine translocation system in *Pseudomonas syringae* pv. tomato DC3000 and its contribution to pathogenicity and fitness. J Bacteriol 187:8450–8461. https://doi.org/10.1128/JB.187.24.8450-8461.2005.
68. Marín M, Pérez-Pantoja D, Donoso RA, Wray V, González B, Pieper DH. 2010. Modified 3-oxoadipate pathway for the biodegradation of methylaromatics in *Pseudomonas reinekei* MT1. J Bacteriol 192:1543–1552. https://doi.org/10.1128/JB.01208-09.
69. Miller JH. 1972. Experiments in molecular genetics. Cold Spring Harbor Laboratory Press, Cold Spring Harbor, NY.
70. Altschul SF, Madden TL, Schaffer AA, Zhang J, Zhang Z, Miller W, Lipman DJ. 1997. Gapped BLAST and PSI-BLAST: a new generation of protein database search programs. Nucleic Acids Res 25:3389–3402. https://doi.org/10.1093/nar/25.17.3389.
71. Marchler-Bauer A, Derbyshire MK, Gonzales NR, Lu S, Chitsaz F, Geer LY, Geer RC, He J, Gwadz M, Hurwitz DI, Lanczycki CJ, Lu F, Marchler GH, Song JS, Thanki N, Wang Z, Yamashita RA, Zhang D, Zheng C, Bryant SH. 2015. CDD: NCBI's conserved domain database. Nucleic Acids Res 43:D222–D226. https://doi.org/10.1093/nar/gku1221.